Available online at www.sciencedirect.com
SCIENCE DIRECT
Biochimica et Biophysica Acta 1758 (2006) 713–720
BIOCHIMICA ET BIOPHYSICA ACTA
BBA
http://www.elsevier.com/locate/bba

# Cellular uptake and subsequent intracellular trafficking of R8-liposomes introduced at low temperature

Akitada Iwasa [a,b], Hidetaka Akita [a,b], Ikramy Khalil [a,b], Kentaro Kogure [a,b], Shiroh Futaki [c,d], Hideyoshi Harashima [a,b,*]

[a] *Graduate School of Pharmaceutical Sciences, Hokkaido University, Sapporo, Hokkaido 060-0812, Japan*
[b] *CREST, Japan Science and Technology Corporation (JST), Japan*
[c] *Institute for Chemical Research, Kyoto University, Uji, Kyoto, Japan*
[d] *PRESTO, Japan Science and Technology Corporation (JST), Japan*

Received 3 November 2005; received in revised form 27 March 2006; accepted 7 April 2006
Available online 5 May 2006

**Abstract**

Intracellular trafficking is a determining factor in the transgene expression efficiency of gene vectors. In the present study, the mechanism of the cellular uptake of octaarginine (R8)-modified liposomes, when introduced at 37 °C and 4 °C, was investigated in living cells. Compared with 37 °C, the uptake of R8-liposomes was only slightly reduced at 4 °C. Dual imaging of liposomes and plasma membranes revealed that R8-liposomes were internalized by vesicular transport, and partially escaped to the cytosol at the perinuclear region at 37 °C. When introduced at 4 °C, intracellular liposomes were observed within a specific region close to the plasma membrane, and internalization of the plasma membrane was completely inhibited. Therefore, at 4 °C, R8-liposomes appear to enter cells via unique pathway, which is separate and distinct from energy-dependent vesicular transport. The subsequent nuclear delivery of encapsulated pDNA, when introduced at 4 °C, was less prominent compared with those introduced at 37 °C. Collectively, these findings demonstrate that a vesicular transport-independent pathway is responsible for the cellular uptake of liposomes. In addition, the uptake route is closely related to the subsequent nuclear delivery process; the operation of an endogenous vesicular sorting system is advantageous for the nuclear delivery of pDNA.


*Keywords:* Intracellular trafficking; PTD; R8; Liposome; Cellular uptake

## 1. Introduction

Improvement in the cellular delivery system for macromolecules is an important issue in the area of drug/gene therapy. Recent studies have revealed that protein transduction domains (PTDs) are promising devices for improving the delivery of various types of biologically active molecules [1,2] such as proteins [3–6], nucleic acids [7–10] and liposomes [11,12]. One of the most widely studied carrier peptide is derived from human immunodeficiency virus-type 1 (TAT) [13,14], which consists of 6 arginine and 2 lysine residues. Based on the high arginine content within the TAT sequence, Futaki et al. synthesized polypeptides that consist solely of arginine residue, and characterized their cellular uptake and intracellular distribution [15–17]. As a result, it was revealed that an octamer of arginine (R8) showed the most efficient internalization. In addition, studies in our laboratory showed that stearylated R8 (STR-R8) was a potent transfection device, which is capable of efficiently delivering plasmid DNA (pDNA) into the cell and even into the nucleus [10,18,19]. Moreover, concerning PTD-modified liposomes, Torchilin et al. compared the cellular uptake of certain types of liposomes, in which TAT-derived PTD was modified on the liposomes with various extents of exposure by means of polyethyleneglycol as a spacer. The findings indicated that liposomes were internalized, only when TAT was displayed on the surface of the liposome so as to readily interact with the cell membrane.

Concerning the mechanism for the uptake of PTD ser se or PTD-modified cargos, initial studies indicated that their uptake was not inhibited by incubation at low temperature, a condition in which

* Corresponding author. Hideyoshi Harashima, Graduate School of Pharmaceutics, Hokkaido University, Sapporo, Hokkaido, 060-0812, Japan. Tel.: +81 11 706 3919; fax: +81 11 706 4879.
*E-mail address:* harasima@pharm.hokudai.ac.jp (H. Harashima).

0005-2736/$ - see front matter © 2006 Elsevier B.V. All rights reserved.
doi:10.1016/j.bbamem.2006.04.015

all of the active cellular uptake is interrupted [11,13,15,20,21]. As a result, it was concluded that PTD-modified cargos were taken up via a vesicular transport-independent pathway (e.g., penetration).

However, a recent report indicated that fixation results in a significant overestimation of cellular uptake and reorganization of intracellular distribution [22]. Because of this, mechanism for the cellular entry has been reexamined using living cells. While current studies found that this process was energy-dependent, the mechanism of internalization of PTDs or PTD-cargos at 37 °C is, however, still controversial, presumably due to differences in the experimental conditions used. Current candidates for the uptake pathway include clathrin-mediated endocytosis [10,22–25], caveolae-mediated endocytosis [26–28] and macropinocytosis [14,17,29]. We recently demonstrated that physiochemical aspects, such as the density of the PTD was a determining factor in sorting the internalization pathway between clathrin-mediated endocytosis and macropinocytosis [30]. Furthermore, the existence of cellular uptake route at low temperature conditions is also a current topic that needs to be examined. Although some reports indicated that cellular uptake is diminished by incubation at 4 °C [10,14,22,28], R8 or heptaarginine modified with a tryptophan residue in the C-terminus (R7W) were reported to be take up by cells even at 4 °C [17,31]. Moreover, confocal images indicate that the intracellular distribution of these peptides were distinct from that taken up at 37 °C. As a result, the possibility of vesicular transport-independent internalization in the case of octaarginine or certain types of PTD peptides cannot be excluded.

The purpose of the present study was to investigate the mechanism of cellular uptake and the subsequent intracellular trafficking of R8-modified liposomes introduced at 37 °C and 4 °C in living cells. To accomplish this, we used recently developed R8-modified liposomes, which are highly associated with the plasma membrane and are efficiently taken up in an in vitro cell culture system [33]. To permit R8 to be displayed on the surface of liposome, it was stearylated, and was then anchored to lipid vesicles via its stearyl moiety. In addition, a condensed pDNA was encapsulated into the R8-liposomes so as to quantitatively evaluate subsequent nuclear delivery by means of TaqMan PCR, in an attempt to address the relationship between the intracellular fate and transgene-expression efficiency.

## 2. Materials and methods

### 2.1. General

Cholesteryl hemisuccinate (CHEMS), cholesterol (Chol), dioleoyl phosphatidyl ethanolamine (DOPE) and Egg yolk phosphatidyl choline (EPC) were purchased from Avanti Polar lipids (Alabaster, AL, USA). Plasmid DNA encoding GFP-luciferase fusion protein (pEGFPluc) was obtained from BD Bioscience Clontech (Palo Alto, CA USA). Rhodamine-labeled transferrin (Rh-Tf) and Sulforhodamine B (S-Rho) was purchased from Molecular Probes (Eugene, OR USA). STR-R8 was synthesized as described previously [18].

### 2.2. Quantification of cellular uptake of liposomes by flow cytometry

The cellular uptake of R8-liposomes and Rh-Tf was assessed by flow cytometry. Liposomes composed of EPC, Chol and STR-R8 (7:3:0.5 molar ratio) were prepared by the hydration method. A lipid film was produced by evaporation of a chloroform solution of 20 μmol lipids with a rotary evaporator under reduced pressure in a round-bottom flask to give a thin film. Hydration buffer (2 ml), PBS containing 1 mM of S-Rho was then added followed by vortexing to hydrate the lipid. Size was controlled by extrusion with a Mini-Extruder (Avanti Polar Lipids), through polycarbonate membrane filters (Nuclepore) with 400, 200 nm pore diameter (11 times each) and 100 nm pore diameter (21 times). Unencapsulated S-Rh was separated on a Bio-Gel A-1.5 m column (100–200 mesh) equilibrated with PBS. For the quantification of cellular uptake, NIH3T3 cells were seeded at a density of $1.0 \times 10^5$ cells per 6-well plate in growth media. After 24 h, the cells were pre-incubated for 30 min at 37 or 4 °C then incubated with R8 liposomes (0.1 mM) or Tf-TMR (tetramethyl rhodamine) (2 μM) in serum free medium for 1 h. Cell surface-bound R8-liposomes were removed as demonstrated previously with minor modifications [23]. Lundberg et al. showed that TAT-GFP, R8-GFP or K8-GFP protein conjugates bound to the cellular surface were nearly completely washed out by a single wash with PBS supplemented with heparin (5 unit/ml) [23]. However, this procedure was not sufficient to completely remove surface-bound R8-liposomes, presumably due to strong binding via its high density of R8-moiety (data not shown). To solve this problem, cells were washed 3 times with ice-cold PBS supplemented with a higher concentration of heparin (20 units/ml) for 3 times. Cellular binding of R8-liposomes encapsulating S-Rho was assessed by confocal laser scanning microscopy. After the incubation of cells with R8-liposomes at 37 °C for 1 h, cell-surface binding of R8-liposomes encapsulating S-Rho were clearly observed without a wash (Fig. 1A). In contrast, after the washing with PBS supplemented with heparin (20 units/ml), cell-surface binding of R8-liposomes were rarely observed as shown in Fig. 1B. Therefore, this condition is adequate for removing cell surface-bound R8-liposomes. For the analysis by flow cytometry, cells were once washed with PBS supplemented with heparin (20 units/ml), and then trypsinized and collected in an eppendorf tube, and then washed two additional times by repeating the precipitation of the cells by centrifugation (1500 rpm, 4 °C, 5 min) and resuspension in 1 ml of heparin-PBS. Finally, cells were suspended in 1 ml of PBS. The cell suspension was then filtered through a nylon mesh to remove cell aggregates and dust, and cells were analyzed with a flow cytometer (FACScan, Becton Dickinson).

### 2.3. Encapsulation of pDNA to the R8-modified liposome

For the quantification of cellular uptake and the nucleus-association of liposomes, plasmid DNA (pDNA) was encapsulated in R8-liposomes as described previously [32]. pDNA (0.1 mg/ml) was then condensed with poly-L-lysine by mixing equal volumes of these solutions at a charge ratio of 2.4 by vortexing at room temperature. After the condensation, a lipid film was produced by evaporation of a chloroform solution with 137.5 nmol of lipid (DOPE/CHEMS=9:2 (molar ratio)) on the bottom of the glass tube. Then, 0.25 ml of the complex solution was added, followed by incubation for 10 min to hydrate the lipids. The final solution of the lipid was 0.55 mM. The hydrated solution was sonicated in a bath-type sonicator (125 W, Branson Ultrasonics, Danbury, CT) to complete the packaging. Finally, the surface of the liposomes was modified with R8 by incubation with a STR-R8 (5 mol% lipids) solution for 30 min at room temperature. Consistent with our previous report, we denote this pDNA-encapsulating R8-liposome as an R8-modified multifunctional envelope-type nano device (R8-MEND) [32].

### 2.4. Quantification of cellular uptake and nucleus—association of pDNA-encapsulating liposomes by TaqMan PCR

For the cellular uptake study, $2 \times 10^5$ cells were seeded on a 6-well cell culture plate for 24 h. The cell culture medium was then replaced with 1 ml of FCS-free media and the suspension was incubated for 30 min at 37 °C or 4 °C. The R8-MEND corresponding to 2 μg of pDNA (24 nmol of total lipid) was added, followed by an additional incubation for 1 h. As a control study, 2 μg of pDNA condensed with LipofectAMINE PLUS (Invitrogen, Carlsbad, California, USA) following the manufacturer's protocol was used. Cells were washed 3 times with PBS supplemented with heparin (20 units/ml) to remove cell surface-bound R8-MEND. To quantify the nuclear association of pDNA, the nuclear fraction was further purified. It is likely that cationic R8-MEND after binding on the cell surface may become redistributed to the outer surface of the nucleus during the purification procedure. To exclude this possibility, all of the purification

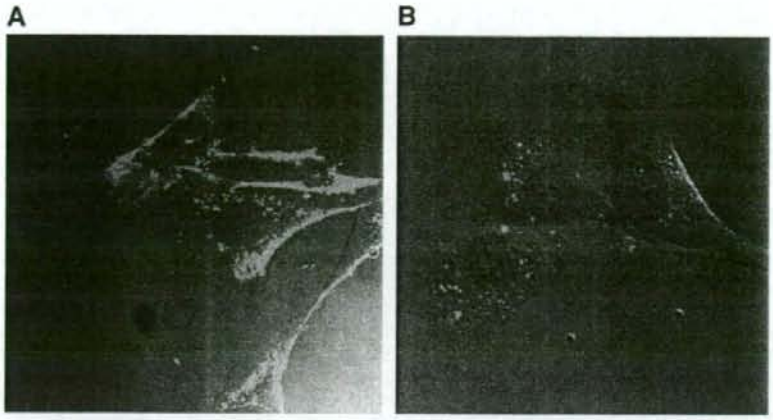


Fig. 1. Heparin-dependent removal of R8-liposomes from cellular surface. R8-liposomes encapsulating S-Rho were incubated for 1 h at 37 °C. Without washing (A), cellular binding of R8-liposomes was observed (arrowhead). After washing with ice-cold PBS supplemented with heparin (20 U/ml) for 3 times (B), cellular binging of

processes were performed in CellScrub buffer (Gene Therapy Systems Inc.), which was originally used for removing the cell surface-bound lipoplex. This reagent is capable of washing out the nuclear surface-bound R8-MEND, and to also interrupt the redistribution of the cytoplasmic R8-MEND to the nuclear fraction during the purification of the nuclei. In fact, after the incubation of R8-MEND and isolation of the nuclei in the presence of CellScrub buffer, the nuclear distribution was negligible (less than 0.1% of applied R8-MEND). The heparin-washed cells were suspended in 375 μl of CellScrub Buffer, and 125 μl of cell lysis solution (2% IGEPAL CA630, 40 mM NaCl, 12 mM $MgCl_2$ and 40 mM Tris–HCl, pH 7.4) was then added. The suspension was centrifuged at 9200×g for 2 min at 4 °C, and the supernatant was removed. This procedure was repeated 3 times. The final pellet was used as the nuclear fraction.

DNA was purified from cell lysates or an isolated nucleus by means of a GenElute Mammalian Genome DNA Miniprep kit (Sigma-Aldrich, St. Louis, MO), and subjected to TaqMan PCR with ABI PRISM® 7700 Sequence Detection System (Applied Biosystems) as reported previously [33]. As a reference, a dilution series of pDNA3.1-GL3 was run along with the samples. The sequence of the probe was 5′-CCGCTGAATTGGAATCCATCTTGCTC-3′ with FAM as a fluorescent dye on the 5′ end and TAMRA as a fluorescence quencher dye at the 3′ end. This probe is designed to anneal to the target between the sense primer (5′-TTGACCGCCTGAAGTCTCTGA-3′) and the antisense primer (5′-ACACCTGCGTCGAAGATGTTG-3′) in the luciferase pDNA sequence. The number of β-actin DNA was also determined by the ABI PRISM® 7700 Sequence Detection System. PCR was performed according to the manufacturer's instructions with 0.5 μM each of the respective forward: 5′-TGCGTGACAT TAAGGAGAAGCTGTG-3′ and reverse: 5′-CAGCGGAACCGCTCATTGC CAATGG-3′ primers, and QuantiTect SYBR Green PCR Master Mix (Qiagen, Hilden, Germany). A linear relationship between the number of cells and the threshold cycle for the β-actin gene amplification was confirmed (data not shown). The amount of nucleus-associated pDNA was normalized by the number of nuclei quantified by the copy number of β-actin DNA.

### 2.5. Imaging of intracellular liposomes by confocal laser scanning microscopy

$1 \times 10^5$ cells were seeded in 2 ml of cell culture medium on a 35 mm/GLASS BASE DISH (IWAKI, Chiba Japan) for 24 h. Plasma membranes were stained with PKH67 GREEN FLUORESCENT CELL LINKER (Sigma-Aldrich; St. Louis, MO USA) following to the protocol with some arrangements. After washing the cells were with serum-free medium, 100 μl of a PKH67 LINKER solution (10 μM) was added, and the cells were further incubated for 5 min at room temperature. The staining reaction was terminated by dilution of medium with 100 μl of serum-free medium. For the imaging of liposomes introduced at 37 °C and 4 °C, the cells were washed 3 times with 1 ml of PBS adjusted to the respective temperature. After washing, R8-liposomes encapsulating sulforhodamine (S-Rho) were immediately added, followed by incubation for 1 h at 37 °C and 4 °C, respectively. The cells were then washed with 1 ml of PBS containing heparin 3 times, and the cell culture medium was exchanged with 1 ml of Krebs-Henseleit Buffer. Confocal images were captured by a Zeiss Axiovert 2000 inverted fluorescence microscope equipped with a 63× NA 1.4 Planachromat objective (Carl Zeiss Co. Ltd., Jena, Germany). During the observation of cells, the temperature of the dish was rigorously controlled by means of a 0 °C~65 °C thermo-control system (Carl Zeiss Co. Ltd.).

### 2.6. Assessment of transfection activity

For the transfection study, $4 \times 10^4$ cells were seeded on a 24-well plate and allowed to stand for 24 h. Before the transfection, the cell culture medium was replaced with 250 μl of serum-free medium, and then incubated for 37 °C or 4 °C for 30 min. R8-MEND corresponding to 0.4 μg pDNA was then added, followed by further incubation for 1 h at 37 °C or 4 °C. After the incubation, the cells were washed with 500 μl of PBS containing 20 units/ml of heparin sulfate 3 times, and heparin-free PBS 1 time. The cells were incubated with 1 ml of DMEM containing 10% fetal calf serum and incubated in a $CO_2$ incubator. At the indicated times, the cells were washed with PBS, and solubilized with reporter lysis buffer (Promega, Madison, WI). The luciferase activity was initiated by the addition of 50 μl of luciferase assay reagent (Promega) into 20 μl of the cell lysate, and measured by means of a luminometer (Luminescencer-PSN, ATTO, Japan). The amount of protein in the cell lysate was determined using a BCA protein assay kit (PIERCE, Rockford, IL).

## 3. Results

### 3.1. Evaluation of the effect of temperature on the cellular uptake of R8-liposomes

The cellular uptake of R8-liposomes encapsulating S-Rho was investigated by flow cytometry at 37 °C and 4 °C. The size and ζ-potential of the prepared liposome are summarized in Table 1. Transferrin (Tf), a common marker of clathrin-dependent endocytosis, was used as a control to evaluate the inhibition of energy-dependent vesicular transport at 4 °C. Without washing the surface-bound liposomes, a comparable or higher degree of cellular association was observed after the incubation at 4 °C compared with that after the incubation at 37 °C (data not

Table 1
The size and ζ potential of prepared liposome

| | Size (nm) | ζ potential (mV) |
|---|---|---|
| R8-liposome | 103.3 ± 11.8 | 37.2 ± 6.8 |
| R8-MEND | 297.9 ± 41.3 | 39.5 ± 12.4 |

The hydrodynamic diameter was measured by quasi-elastic light scattering by means of an electrophoresis light scattering spectrophotometer.

shown). As shown in Fig. 1, the heparin wash efficiently removed the cell surface bound of R8-liposomes (see Materials and methods). Even after the removal of surface bound liposomes, a FACS analysis revealed that the internalization of R8-liposomes was only slightly inhibited at the low temperature used (Fig. 2A), while the internalization of Tf was significantly inhibited (Fig. 2B). The mean fluorescence intensity of 10,000 analyzed cells is shown in Fig. 2C. Approximately 80% of the cellular uptake of R8-liposomes was retained, even at 4 °C, while uptake of Tf was drastically decreased to approximately 30%.

To quantify cellular uptake and following nuclear delivery by TaqMan PCR, plasmid DNA was also encapsulated in the R8-liposome. Here, we denote this liposome as R8-MEND, consistent with a previous report [32]. Compared with R8-liposomes encapsulating S-Rho, the size of the R8-MEND was approximately 3-times larger (Table 1). The cellular uptake of the R8-MEND at low temperature was also confirmed (Fig. 3). As a control, pDNA condensed by LipofectAMINE PLUS, a commercially available cationic liposome was used, since it was previously reported that its internalization was severely inhibited at low temperature [19]. Consistent with the results obtained with the R8-liposome, a major portion (>50%) of the cellular uptake of R8-MEND was retained even by incubation at 4 °C, where the uptake of lipoplex was diminished to less than 30%.

### *3.2. Mechanism of uptake of R8-liposomes introduced at 37 °C and 4 °C*

The involvement of vesicular transport in the cellular uptake of R8-liposomes was investigated by means of dual imaging of

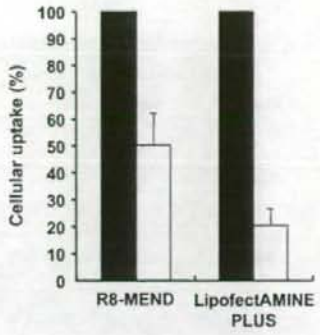


Fig. 3. Quantitative comparison of the uptake of R8-MEND introduced at 37 °C and 4 °C. NIH3T3 cells were incubated with the R8-MEND at 37 °C and 4 °C for 1 h to evaluate cellular uptake. Uptake was quantified in terms of the number of copies of luciferase genes by TaqMan-PCR. Closed and open bar represents cellular uptake of pDNA quantified by TaqMan PCR after the incubation at 37 °C and 4 °C, respectively. Cellular association was normalized by the number of cells, which is quantified by the number of copies for genomic β-actin gene.

an R8-liposome encapsulating S-Rho and PKH67-labeled plasma membrane. After incubation at 37 °C for 1 h, the major fraction of the R8-liposomes was co-localized with intracellular vesicular structures, suggesting that R8-liposomes are mainly taken up to the cells by vesicular transport (Fig. 4A). Some liposomes were detected as red clusters close to the nucleus, suggesting that liposomes were partially released from the vesicular compartment. When incubated at 4 °C, the fluorescence signals of PKH67 were dominantly detected on the surface of the cells, suggesting that the vesicular transport system was severely interrupted under these conditions (Fig. 4B), whereas a small number of green clusters were still observed just beneath the plasma membrane. Even under these conditions, the fluorescence signal of S-Rho was detected in the intracellular region. Magnified images further reveled that intracellular signals corresponding to S-Rho (indicated as red arrowheads in Fig. 4B; inset 1) were detected close to the green signals derived from the PKH67 signal (indicated as green arrowheads in Fig. 4B; inset 1), but were not colocalized with each other. In this case,

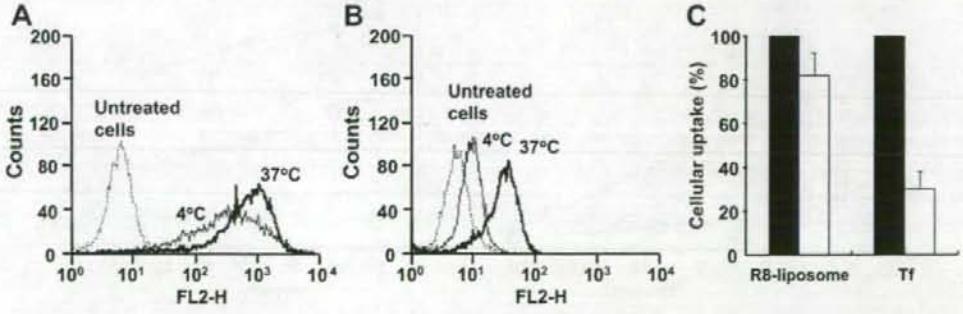


Fig. 2. Quantitative comparison of the uptake of R8-liposomes introduced at 37 °C and 4 °C. R8-liposomes encapsulating S-Rho (A) and Rho-Tf (B) were incubated with NIH3T3 cells in serum free medium for 1 h. After washing with 20 U/ml of heparin, the cells were detached by treatment with a trypsin solution. Cells were collected by centrifugation, and resuspended in 100 μl of PBS. The cells were analyzed with a flow cytometer, and the mean fluorescence was then plotted (C). Thick and thin lines represent the cellular uptake of R8-liposomes introduced at 37 °C and 4 °C (A and B). Hatched lines represent the non-treated control. (C) Closed and open bar represents mean fluorescence of analyzed 10000 cells after the incubation at 37 °C and 4 °C, respectively.

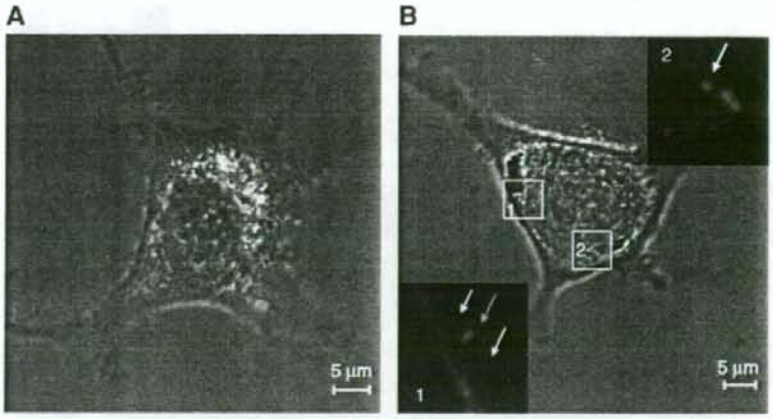


Fig. 4. Dual imaging of the R8-liposome encapsulating S-Rho and plasma membrane labeled with PKH67. After staining the plasma membrane with PKH67, R8-liposomes encapsulating S-Rho were immediately added, followed by incubation for 1 h at 37 °C (A) and 4 °C (B), respectively. Fluorescence images were captured by means of confocal laser scanning microscopy. During the observation of images, the temperature of the dish was rigorously controlled by 37 °C or 4 °C by a thermo-control system. The white and red arrowhead in (B; inset 1 and 2, respectively) indicates intracellular R8-liposomes taken up at 4 °C. Green arrowhead in inset 2 represented intracellular PKH67 signals.

R8-liposomes may be taken up via temperature-independent invagination, followed by their rapid escape to the cytosol. Moreover, some red signals were far away from the green signals (Fig. 4B; inset 2). This indicates that the R8-liposomes were alternatively internalized via vesicular transport-independent pathway. Confocal images also revealed that R8-liposomes were localized close to the plasma membrane (Fig. 3B: arrowhead), but were not localized on peri-nuclear region.

### *3.3. Nuclear association and trans-gene expression of R8-MEND introduced at 37 °C and 4 °C*

The nuclear association of R8-MEND after the internalization at 37 °C and 4 °C (denoted as R8-MEND$_{37}$ and R8-MEND$_4$) was quantified by means of TaqMan PCR (Fig. 5A). After the incubation of R8-MEND for 1 h at 37 °C and 4 °C, the cells were washed with a heparin solution to remove cell surface-bound R8-MEND, and further incubated at 37 °C for the indicated times. The nuclei were fractionated, and nucleus-associated pDNA was subsequently quantified by TaqMan PCR. A peak for the nuclear association of R8-MEND$_{37}$ appeared within 3 h, while the peak for R8-MEND$_4$ was observed at 6 h. These data indicate that the R8-MEND$_{37}$ reached the nucleus more rapidly than R8-MEND$_4$. The percent of nucleus-associated pDNA to the totally internalized one ($F_{nuc}$) is summarized in Table 2. Comparing the $F_{nuc}$ at the time of peaking (at 3 h for the R8-MEND$_{37}$ versus at 6 h for the R8-MEND$_4$), the R8-MEND$_{37}$ showed an approximately 4.6 times higher value than that of R8-MEND$_4$. (24.8% vs. 5.43%). Collectively, R8-MEND$_{37}$ was able to gain access to the nucleus more rapidly and more efficiently compared with the R8-MEND$_4$.

To compare the transgene expression between R8-MEND$_{37}$ and R8-MEND$_4$, cells were incubated at 37 °C for the indicated

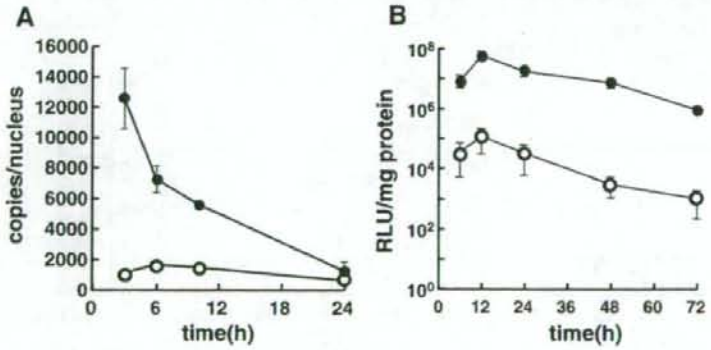


Fig. 5. Time profiles for the nuclear associating pDNA and transfection activity after the introduction of R8-MEND at 37 °C and 4 °C. (A) After the introduction of R8-MEND at 37 °C and 4 °C, cells were washed with heparin to remove the membrane-bound R8-MEND. Nucleus-associated pDNA was quantified by nuclear fractionation followed by TaqMan PCR. The number of the nucleus-associated pDNA was normalized by the number of nucleus quantified by the copy number of β-actin genome. (B) Transfection activity of R8-MEND introduced at 37 °C and 4 °C at the indicated times. The results obtained for the incubation at 37 °C and 4 °C are represented as closed and open circle, respectively. The vertical axis represents luciferase activity expressed as relative light units (RLU)/mg protein.

times after washing with a heparin sulfate (Fig. 5B). At all the indicated times, the transgene-expression of the R8-MEND$_{37}$ was 2- or 3- orders of magnitude higher than that for the R8-MEND$_4$. It should be noted that the transfection activity of the R8-MEND incubated at 37 °C and 4 °C was comparable, when the cell surface-bound R8-MEND was not removed by heparin sulfate treatment (data not shown). This strongly suggests that the intracellular trafficking of R8-MEND introduced in the cells at 4 °C was distinct from that of the plasma membrane-bound R8-MEND after cell culture medium was warmed from 4 °C to 37 °C. The amount of protein in the wells showed quite comparable values between R8-MEND$_{37}$ and R8-MEND$_4$ (data not shown). Therefore, the prominent difference in transgene expression cannot be accounted for by cytotoxic effects during the incubation at 4 °C. Finally, "transgene expression normalized by nuclear pDNA" was compared at two time points (Table 3) [34]. At 6 h, R8-MEND$_{37}$ exhibited dramatically higher values (51-fold) compared with that of R8-MEND$_4$. Moreover, at 24 h, the difference was greater (247-fold). These data suggest that the intrinsic activity of pDNA to produce a gene product was significantly impaired, when introduced by R8-MEND$_4$ compared with that introduced by R8-MEND$_{37}$.

## 4. Discussion

Recent studies have indicated that vesicular transport plays an important role in the cellular uptake of PTD-modified cargos [10,14,17,22–29]. Inhibitors and/or biomarkers for various vesicular transport systems were used in attempt to identify the pathway responsible for cellular uptake. These studies revealed that clathrin-mediated endocytosis [22,23,30], macropinocytosis [14,17,29,30] and caveolae-mediated endocytosis [26] are all involved in the uptake of PTD peptides ser se, or PTD-modified proteins, while major determining factor in sorting the internalization pathway remains obscure. Vesicular transports are driven by coupling with ATP hydrolysis. Therefore, these pathways should be inhibited at low temperatures. In fact, the cellular uptake of transferrin was drastically inhibited to approximately 30%. In the present study, the majority of R8-liposomes were taken up by cells, even at 4 °C. Initial studies indicated that PTD is able to penetrate the cells via endocytosis-independent pathways since cellular uptake was unaffected by low-temperature incubation and with endocytosis inhibitors [13]. Whereas these results were artifacts resulting from cell fixation [22], recent studies using living cells still support the internalization of a certain kind of PTD even at the low temperature

Table 2
Efficiency of nuclear association of R8-MEND37 and R8-MEND to the totally internalized MENDS

| | Uptake (copies/cell) | Percent of nuclear association of pDNA to the total cellular uptake | | | |
|---|---|---|---|---|---|
| | | 3 h | 6 h | 10 h | 24 h |
| 37 °C | $5.05 \times 10^4$ | 24.8 | 14.3 | 11.1 | 2.40 |
| 4 °C | $2.96 \times 10^4$ | 3.53 | 5.43 | 4.82 | 1.91 |

The efficiency of nuclear association was represented as a percent of nuclear association of pDNA to the total cellular uptake.

Table 3
Comparison of the transfection efficiency normalized by nuclear pDNA transfected by R8-MEND$_{37}$ and R8-MEND$_4$

| | Time post-injection (h) | |
|---|---|---|
| | 6 h | 24 h |
| 37 °C | $1.18 \times 10^3$ | $1.45 \times 10^4$ |
| 4 °C | 23.1 | 58.5 |

Transfection activity and nuclear pDNA at 6 h and 24 h was based on Fig. 5A and B, respectively. Values are expressed as RLU/mg protein/copy.

[17,31]. Nakase et al., quantitatively compared the cellular uptake of R8 by the incubation at 37 °C and 4 °C, and found that approximately 60–70% of the cellular uptake of R8 was retained on incubation at 4 °C [17]. This is consistent with our findings showing that approximately 80% and 50% of the cellular uptake of R8-liposomes and R8-MEND was retained, on incubation at 4 °C (Figs. 2 and 3).

In contrast to the mechanism for cellular uptake at 37 °C, very little information is available concerning the uptake at 4 °C. The involvement of non-vesicular transport in the uptake of R8-liposomes was further investigated by the dual labeling of plasma membranes with PKH67 and S-Rho encapsulated in the liposomes (Fig. 3). Since PKH67 stably incorporates a fluorescent dye into the lipid regions of cell membranes with its long aliphatic tail, all of the internalized vehicles after the membrane staining should be labeled irrespective of the internalization pathway. In this observation, the temperature of the dish was carefully kept by means of a thermo-control system, and cell surface-bound R8-liposomes were removed by treatment with a heparin sulfate solution in order to exclude the possibility that cell-surface bound R8-liposomes during the incubation at 4 °C were internalized via an energy-dependent vesicular transport system by temporal and local warming caused by laser irradiation. As a result, internalization of plasma membranes labeled with PKH67 was rarely observed at 4 °C (Fig. 4B). Even in this condition, the internalization of R8-liposome was observed in the cytoplasm, suggesting that the R8-liposome probably penetrated into the cells even at 4 °C. Furthermore, the localization of R8-liposomes were restricted to a specific areas in close proximity to plasma membrane (Fig. 4B: insets 1 and 2), as was also observed for the R8 peptide [17]. This suggested that migration of R8-liposomes taken up at low temperature was severely restricted.

It has been proposed that guanidinium-rich peptides interact with negatively charged, bidentate hydrogen bond acceptor groups of endogenous membrane constituents, forming a membrane-soluble ion pair complex, which then migrates into the lipid bilayer [35]. However, this hypothesis was only applied to small molecules (MW ca. < 3000). An alternative pathway such as temperature-insensitive potocytosis [36] may be responsible for the translocation of R8-liposomes after the formation of ion pairs. The temperature-insensitive invagination is supported by the fact that some PKH-67 signals were observed in the intracellular region, but were restricted to directly beneath the plasma membrane (indicated as green arrowheads in Fig. 4B; inset 1). Furthermore, a part of intracellular R8-liposomes were detected close to the PKH-67 signal (indicated as red arrowhead in Fig. 4B; inset 1). These findings suggest that R8-liposomes

were partially taken up by temperature-insensitive potocytosis, followed by rapid release to the cytosol. In addition, some R8 liposomes were detected in the intracellular region away from the PKH67 signal (indicated as white arrowhead in Fig. 4B; inset 2), suggesting that alternative mechanism such as penetration may also play a role. The cellular uptake of R8-MEND was more temperature-sensitive compared to the R8-liposome (50% vs. 20% inhibition) as shown in Figs. 2C and 3. Since the mean diameter of the R8-MEND was significantly larger than that of R8-liposomes (Table 1), smaller sized of macromolecules may be more acceptable to these temperature-independent cellular uptake mechanisms. An investigation of molecular mechanism for the cellular uptake is ongoing in our laboratory.

In the 37 °C incubation, R8-liposomes, free from the co-localization with plasma membranes, were observed at the perinuclear region, which is distinct from the localization of R8-liposomes incubated at 4 °C. These liposomes could then be transported to the perinuclear region by intracellular sorting by vesicular trafficking, and then released to the cytosol. Some recent studies indicated that the endosomal escape of PTD is inhibited by ammonium chloride [25] or chroloquine [37]. Thus, it is possible that the endosomal escape of R8-liposomes is coupled with acidification in the vesicular compartment. In this sense, clathrin-mediated endocytosis [22] or macropinocytosis [23] is a more plausible uptake pathway for the R8-liposomes compared with caveolae-mediated endocytosis [26], since the pH in caveolae does not decrease after invagination. In fact, we have demonstrated that cellular uptake R8-liposomes used in the present study were inhibited by amiloride, which is a inhibitor of the macropinocytosis [30].

Considering the relationship between intracellular fate and time profiles for nuclear association, the findings strongly suggest that the involvement of vesicular transport to the peri-nuclear region is advantageous for the rapid and efficient nuclear delivery of R8-MEND introduced at 37 °C (Fig. 5A and Table 2). As mentioned above, R8-$MEND_{37}$ appears to be released from vesicular compartments that are close to the nucleus after active vesicular transport, while R8-$MEND_4$ appears to be directly introduced to the cytoplasm in close proximity to the plasma membrane. Therefore, R8-$MEND_4$ needs to travel longer distance in the cytoplasm to reach the nucleus compared with the R8-$MEND_{37}$. It has been reported that the movement of macromolecules in the cytoplasm is severely restricted [38]. If this is true, then, the speed and efficiency of R8-liposomes for reaching the nucleus is closely related to the distance from the cytoplasmic R8-liposome to the nucleus. In fact, Daum et al., indicated that the trans-gene expression of pDNA microinjected into the cytoplasm far from the nucleus was much lower than that injected close to the nucleus.

Finally, time profiles for the transgene expression were evaluated. At 37 °C, transgene expression was peaked at 12 h and then decreased slightly (approximately 30% of the peak luciferase activity) at 24 h, which is inconsistent with the fact that nuclear pDNA peaked at 3 h and then decreased monotonically. The synthesis of proteins is a product of the nuclear transcription of pDNA and subsequent translation. As a result, time lag between peak of nuclear pDNA (within 3 h) and luciferase activity (12 h) may be derived from the time required for the nuclear transcription and translation. Concerning the elimination process, a decrease in transgene expression from 12 h to 24 h was less prominent than that of nuclear pDNA. Since the apparent luciferase activity is balanced by synthesis and clearance of gene products, the inefficient clearance of a gene product may reflect the moderate luciferase activity, even though biosynthesis may be reduced in response to the time-dependent decrease in nuclear pDNA. In this sense, "transgene expression normalized by nuclear pDNA" calculated as the trans-gene expression divided by the gene copies in the nucleus (Table 3) is not necessarily a direct index of intrinsic activity of pDNA for the biosynthesis. However, if the intrinsic activity of pDNA to produce the gene product was comparable between R8-$MEND_{37}$ and R8-$MEND_4$, "transgene expression normalized by nuclear pDNA" (Table 3) may represent comparable values based on the hypothesis that the clearance of a gene product should be comparable regardless of the conditions used for the introducing the R8-MEND. R8-$MEND_{37}$ exhibited approximately a 500 times higher trans-gene expression compared with R8-$MEND_4$ (Fig. 5B). In comparing "transgene expression normalized by nuclear pDNA", R8-$MEND_{37}$ shows 2- or 3 orders of magnitude higher values than those of R8-$MEND_4$ (Table 3). As mentioned in Materials and methods, the core particle of pDNA condensed with polycations was coated with a lipid envelope (DOPE/CHEMS, a pH sensitive fusogenic lipid composition [39,40]) to form the MEND structure [32]. It has been demonstrated that trans-gene expression after the nuclear microinjection of pDNA is strongly impaired when it is injected in the form of a lipoplex [41,42], suggesting that pDNA should be free from cationic lipid components so as to be efficiently recognized by intra-nuclear transcription factors. When R8-$MEND_{37}$ escapes from the vesicular compartment, the lipid envelope is presumably consumed by fusion with the cellular membrane, forming a hexagonal structure-II structure in response to the low intra-vesicular pH [43]. As a result, pDNA encapsulated in an R8-$MEND_{37}$ may be more prominently subject to the transcription process compared with that in the R8-$MEND_4$.

Collectively, it was verified that R8-liposomes, when incubated at a temperature of 4 °C, enter cells via a unique pathway distinct from that introduced at 37 °C, whereas subsequent nuclear delivery was less efficient compared with that of R8-liposomes introduced at a temperature of 37 °C. This conclusion provides encouragement for using a strategy involving the endogenous vesicular sorting system for the nuclear targeting of macromolecules.

## Acknowledgements

This work was supported in part by Grants-in-Aid for Scientific Research (B) and Grant-in-Aid for Young Scientists (B) from the Ministry of Education, Culture, Sports, Science and Technology of Japan, and by Grants-in-Aid for Scientific Research on Priority Areas from the Japan Society for the Promotion of Science.

## References

[1] H. Brooks, B. Lebleu, E. Vives, Tat peptide-mediated cellular delivery: back to basics, Adv. Drug Deliv. Rev. 57 (2005) 559–577.

[2] B. Gupta, T.S. Levchenko, V.P. Torchilin, Intracellular delivery of large molecules and small particles by cell-penetrating proteins and peptides, Adv. Drug Deliv. Rev. 57 (2005) 637–651.
[3] S.R. Schwarze, A. Ho, A. Vocero-Akbani, S.F. Dowdy, In vivo protein transduction: delivery of a biologically active protein into the mouse, Science 285 (1999) 1569–1572.
[4] M. Lindgren, X. Gallet, U. Soomets, M. Hallbrink, E. Brakenhielm, M. Pooga, R. Brasseur, U. Langel, Translocation properties of novel cell penetrating transportan and penetratin analogues, Bioconjug. Chem. 11 (2000) 619–626.
[5] S. Fawell, J. Seery, Y. Daikh, C. Moore, L.L. Chen, B. Pepinsky, J. Barsoum, Tat-mediated delivery of heterologous proteins into cells, Proc. Natl. Acad. Sci. U. S. A. 91 (1994) 664–668.
[6] A.M. Vocero-Akbani, N.V. Heyden, N.A. Lissy, L. Ratner, S.F. Dowdy, Killing HIV-infected cells by transduction with an HIV protease-activated caspase-3 protein, Nat. Med. 5 (1999) 29–33.
[7] A. Astriab-Fisher, D.S. Sergueev, M. Fisher, B.R. Shaw, R.L. Juliano, Antisense inhibition of P-glycoprotein expression using peptide-oligonucleotide conjugates, Biochem. Pharmacol. 60 (2000) 83–90.
[8] M.C. Morris, L. Chaloin, F. Heitz, G. Divita, Translocating peptides and proteins and their use for gene delivery, Curr. Opin. Biotechnol. 11 (2000) 461–466.
[9] E.L. Snyder, S.F. Dowdy, Protein/peptide transduction domains: potential to deliver large DNA molecules into cells, Curr. Opin. Mol. Ther. 3 (2001) 147–152.
[10] I.A. Khalil, S. Futaki, M. Niwa, Y. Baba, N. Kaji, H. Kamiya, H. Harashima, Mechanism of improved gene transfer by the N-terminal stearylation of octaarginine: enhanced cellular association by hydrophobic core formation, Gene Ther. 11 (2004) 636–644.
[11] V.P. Torchilin, R. Rammohan, V. Weissig, T.S. Levchenko, TAT peptide on the surface of liposomes affords their efficient intracellular delivery even at low temperature and in the presence of metabolic inhibitors, Proc. Natl. Acad. Sci. U. S. A. 98 (2001) 8786–8791.
[12] C. Marty, C. Meylan, H. Schott, K. Ballmer-Hofer, R.A. Schwendener, Enhanced heparan sulfate proteoglycan-mediated uptake of cell-penetrating peptide-modified liposomes, Cell. Mol. Life Sci. 61 (2004) 1785–1794.
[13] E. Vives, P. Brodin, B. Lebleu, A truncated HIV-1 Tat protein basic domain rapidly translocates through the plasma membrane and accumulates in the cell nucleus, J. Biol. Chem. 272 (1997) 16010–16017.
[14] J.S. Wadia, R.V. Stan, S.F. Dowdy, Transducible TAT-HA fusogenic peptide enhances escape of TAT-fusion proteins after lipid raft macropinocytosis, Nat. Med. 10 (2004) 310–315.
[15] S. Futaki, T. Suzuki, W. Ohashi, T. Yagami, S. Tanaka, K. Ueda, Y. Sugiura, Arginine-rich peptides. An abundant source of membrane-permeable peptides having potential as carriers for intracellular protein delivery, J. Biol. Chem. 276 (2001) 5836–5840.
[16] T. Suzuki, S. Futaki, M. Niwa, S. Tanaka, K. Ueda, Y. Sugiura, Possible existence of common internalization mechanisms among arginine-rich peptides, J. Biol. Chem. 277 (2002) 2437–2443.
[17] I. Nakase, M. Niwa, T. Takeuchi, K. Sonomura, N. Kawabata, Y. Koike, M. Takehashi, S. Tanaka, K. Ueda, J.C. Simpson, A.T. Jones, Y. Sugiura, S. Futaki, Cellular uptake of arginine-rich peptides: roles for macropinocytosis and actin rearrangement, Mol. Ther. 10 (2004) 1011–1022.
[18] S. Futaki, W. Ohashi, T. Suzuki, M. Niwa, S. Tanaka, K. Ueda, H. Harashima, Y. Sugiura, Stearylated arginine-rich peptides: a new class of transfection systems, Bioconjug. Chem. 12 (2001) 1005–1011.
[19] H. Akita, R. Ito, I.A. Khalil, S. Futaki, H. Harashima, Quantitative three-dimensional analysis of the intracellular trafficking of plasmid DNA transfected by a nonviral gene delivery system using confocal laser scanning microscopy, Mol. Ther. 9 (2004) 443–451.
[20] D. Derossi, A.H. Joliot, G. Chassaing, A. Prochiantz, The third helix of the Antennapedia homeodomain translocates through biological membranes, J. Biol. Chem. 269 (1994) 10444–10450.
[21] D. Derossi, S. Calvet, A. Trembleau, A. Brunissen, G. Chassaing, A. Prochiantz, Cell internalization of the third helix of the Antennapedia homeodomain is receptor-independent, J. Biol. Chem. 271 (1996) 18188–18193.
[22] J.P. Richard, K. Melikov, E. Vives, C. Ramos, B. Verbeure, M.J. Gait, L.V. Chernomordik, B. Lebleu, Cell-penetrating peptides. A reevaluation of the mechanism of cellular uptake, J. Biol. Chem. 278 (2003) 585–590.
[23] M. Lundberg, S. Wikstrom, M. Johansson, Cell surface adherence and endocytosis of protein transduction domains, Mol. Ther. 8 (2003) 143–150.
[24] S. Console, C. Marty, C. Garcia-Echeverria, R. Schwendener, K. Ballmer-Hofer, Antennapedia and HIV transactivator of transcription (TAT) "protein transduction domains" promote endocytosis of high molecular weight cargo upon binding to cell surface glycosaminoglycans, J. Biol. Chem. 278 (2003) 35109–35114.
[25] T.B. Potocky, A.K. Menon, S.H. Gellman, Cytoplasmic and nuclear delivery of a TAT-derived peptide and a beta-peptide after endocytic uptake into HeLa cells, J. Biol. Chem. 278 (2003) 50188–50194.
[26] A. Ferrari, V. Pellegrini, C. Arcangeli, A. Fittipaldi, M. Giacca, F. Beltram, Caveolae-mediated internalization of extracellular HIV-1 tat fusion proteins visualized in real time, Mol. Ther. 8 (2003) 284–294.
[27] A. Fittipaldi, A. Ferrari, M. Zoppe, C. Arcangeli, V. Pellegrini, F. Beltram, M. Giacca, Cell membrane lipid rafts mediate caveolar endocytosis of HIV-1 Tat fusion proteins, J. Biol. Chem. 278 (2003) 34141–34149.
[28] A. Eguchi, T. Akuta, H. Okuyama, T. Senda, H. Yokoi, H. Inokuchi, S. Fujita, T. Hayakawa, K. Takeda, M. Hasegawa, M. Nakanishi, Protein transduction domain of HIV-1 Tat protein promotes efficient delivery of DNA into mammalian cells, J. Biol. Chem. 276 (2001) 26204–26210.
[29] I.M. Kaplan, J.S. Wadia, S.F. Dowdy, Cationic TAT peptide transduction domain enters cells by macropinocytosis, J. Control. Release 102 (2005) 247–253.
[30] I.A. Khalil, K. Kogure, S. Futaki, H. Harashima, High density of octaarginine stimulates macropinocytosis leading to efficient intracellular trafficking for gene expression, J. Biol. Chem. 281 (2006) 3544–3551.
[31] P.E. Thoren, D. Persson, P. Isakson, M. Goksor, A. Onfelt, B. Norden, Uptake of analogs of penetratin, Tat(48–60) and oligoarginine in live cells, Biochem. Biophys. Res. Commun. 307 (2003) 100–107.
[32] K. Kogure, R. Moriguchi, K. Sasaki, M. Ueno, S. Futaki, H. Harashima, Development of a non-viral multifunctional envelope-type nano device by a novel lipid film hydration method, J. Control. Release 98 (2004) 317–323.
[33] S. Hama, H. Akita, R. Ito, H. Mizuguchi, T. Hayakawa, H. Harashima, Quantitative comparison of intracellular trafficking and nuclear transcription between adenoviral and lipoplex systems, Mol. Ther. 13 (2006) 786–794.
[34] H. Ochiai, H. Harashima, H. Kamiya, Intranuclear disposition of exogenous DNA in vivo: silencing, methylation and fragmentation, FEBS Lett. 580 (2006) 918–922.
[35] J.B. Rothbard, T.C. Jessop, P.A. Wender, Adaptive translocation: the role of hydrogen bonding and membrane potential in the uptake of guanidinium-rich transporters into cells, Adv. Drug Deliv. Rev. 57 (2005) 495–504.
[36] R.G. Anderson, B.A. Kamen, K.G. Rothberg, S.W. Lacey, Potocytosis: sequestration and transport of small molecules by caveolae, Science 255 (1992) 410–411.
[37] R. Fischer, K. Kohler, M. Fotin-Mleczek, R. Brock, A stepwise dissection of the intracellular fate of cationic cell-penetrating peptides, J. Biol. Chem. 279 (2004) 12625–12635.
[38] G.L. Lukacs, P. Haggie, O. Seksek, D. Lechardeur, N. Freedman, A.S. Verkman, Size-dependent DNA mobility in cytoplasm and nucleus, J. Biol. Chem. 275 (2000) 1625–1629.
[39] J. Connor, L. Huang, Efficient cytoplasmic delivery of a fluorescent dye by pH-sensitive immunoliposomes, J. Cell Biol. 101 (1985) 582–589.
[40] R. Tachibana, H. Harashima, M. Shono, M. Azumano, M. Niwa, S. Futaki, H. Kiwada, Intracellular regulation of macromolecules using pH-sensitive liposomes and nuclear localization signal: qualitative and quantitative evaluation of intracellular trafficking, Biochem. Biophys. Res. Commun. 251 (1998) 538–544.
[41] H. Pollard, J.S. Remy, G. Loussouarn, S. Demolombe, J.P. Behr, D. Escande, Polyethylenimine but not cationic lipids promotes transgene delivery to the nucleus in mammalian cells, J. Biol. Chem. 273 (1998) 7507–7511.
[42] J. Zabner, A.J. Fasbender, T. Moninger, K.A. Poellinger, M.J. Welsh, Cellular and molecular barriers to gene transfer by a cationic lipid, J. Biol. Chem. 270 (1995) 18997–19007.
[43] Y. Xu, F.C. Szoka Jr., Mechanism of DNA release from cationic liposome/DNA complexes used in cell transfection, Biochemistry 35 (1996) 5616–5623.

# Delivery of Condensed DNA by Liposomal Non-viral Gene Delivery System into Nucleus of Dendritic Cells

Takashi NAKAMURA,[a,b] Rumiko MORIGUCHI,[a,b] Kentaro KOGURE,*[a,b] Arisa MINOURA,[a] Tomoya MASUDA,[a,b] Hidetaka AKITA,[a,b] Kazunori KATO,[c] Hirofumi HAMADA,[c] Masaharu UENO,[d] Shiroh FUTAKI,[e,f] and Hideyoshi HARASHIMA[a,b]

[a] *Graduate School of Pharmaceutical Sciences, Hokkaido University; Kita 12, Nishi 6, Kita-ku, Sapporo 060–0812, Japan:* [b] *CREST and* [f] *PRESTO, Japan Science and Technology Agency (JST); 3–1–6 Shibuya, Shibuya-ku, Tokyo 150–0002, Japan:* [c] *Department of Molecular Medicine, Sapporo Medical University; Minami 1 Nishi 17, Chuo-ku, Sapporo 060–8556, Japan:* [d] *Faculty of Pharmaceutical Sciences, University of Toyama; 2630 Sugitani, Toyama 930–0194, Japan: and* [e] *Institute for Chemical Research, Kyoto University; Uji, Kyoto 611–0011, Japan.*
Received February 14, 2006; accepted March 2, 2006; published online March 3, 2006

**In this study, we developed novel double-membranous non-viral gene delivery system modified with SV-40 T antigen-derived nuclear localization signal (NLS-DMEND) for delivery of luciferase plasmid DNA to nucleus of non-dividing mouse bone marrow-derived dendritic cells (BMDC). Intracellular trafficking and gene expression of NLS-DMEND in the BMDC were evaluated. Condensed DNA was observed in the nucleus by confocal laser scanning microscopy, and the NLS-DMEND induced significant luciferase activity in the BMDC. It was suggested that the condensed DNA particle transferred into nucleus via energy dependent manner, since the nuclear transfer was inhibited by metabolic inhibitors. In conclusion, condensed plasmid DNA was delivered into the nucleus of non-dividing BMDC by NLS-DMEND.**

**Key words** non-viral gene delivery system; non-dividing cell; nuclear localization signal; nuclear transfer

In general, foreign substances can not enter the nucleus of non-dividing cells, in which nuclear membrane does not disappear by cell division, since nuclear transfer is strictly controlled by precise machinery. For example, nuclear proteins are recognized by importin $\alpha$ in the cytoplasm with a nuclear localization signal (NLS) attached to the nuclear proteins, and importin $\beta$ then combines with the NLS/importin $\alpha$. The complex binds to the nuclear pore complex (NPC), and passes through the NPC into nucleus.[1] Therefore, it is difficult to transfer foreign plasmid DNA (pDNA) into the nucleus of a non-dividing cell by means of an artificial gene delivery system such as cationic liposomes or cationic polymers.[2–6]

Many researchers have attempted to artificially transfer pDNA utilizing nuclear transport machinery, *i.e.*, the nuclear transfer of electrostatic complexes between NLS and DNA,[7–10] NLS-conjugated DNA, *etc.*[11–16] We also synthesized NLS conjugated linear pDNA and evaluated its nuclear transfer by a microinjection technique, but, no increase in the nuclear transport of pDNA was observed.[17] This result suggests that a positively charged NLS is not able to function due to electrostatic interactions with the negatively charged DNA. Therefore, it is possible that steric flexibility in the NLS is necessary for an interaction with importin.

In this study, we attempted to transfer pDNA condensed by a cationic peptide protamine into the nucleus of non-dividing mouse bone marrow derived dendritic cells (BMDC) using an NLS-modified liposomal non-viral gene delivery system (NLS-DMEND), of which NLS peptide was presented on the surface to retain its flexibility. We evaluated intracellular trafficking and the gene expression of the NLS-DMEND to evaluate its nuclear transfer capabilities. In addition, we examined the effect of metabolic inhibitors to confirm the energy dependency of the nuclear transfer of pDNA by the NLS-DMEND.

## MATERIALS AND METHODS

**Materials** Dioleoyl phosphatidylethanolamine (DOPE) and *N*-(7-nitro-2-1,3-benzoxadiazol-4-yl)-DOPE (NBD-DOPE) were purchased from AVANTI Polar Lipids Inc (Alabaster, AL, U.S.A.). Cholesteryl hemisuccinate (CHEMS) was obtained from SIGMA-Aldrich Co. (St. Louis, MO, U.S.A.). Protamine sulfate salmon milt was purchased from Merck KGaA (Darmstadt, Germany). The pDNA pCMV-luc (7037 bp) encoding luciferase was prepared by EndFree Plasmid Mega Kit (Qiagen GmbH, Hilden, Germany). The peptides used in this study were synthesized as previously reported.[18] NIH3T3 and HeLa cells were obtained from the American Type Culture Collection (Manassas, VA, U.S.A.).

**Preparation of Bone Marrow-Derived Dendritic Cells (BMDC) of Mice** BMDC were prepared based on a previously reported method[19,20] with some modifications. BM cells were treated with antibodies and rabbit complement to remove natural killer cells, B-lymphocytes, T-lymphocytes and granulocytes. The remaining BM cells were then cultured in RPMI 1640 medium containing 50 $\mu$M 2-mercaptoethanol, 10 mM HEPES, 1 mM sodium pyruvate, 100 unit/ml penicillin–streptomycin, 10 ng/ml GM-CSF and 10% FCS. On day 2 and day 4, non-adherent cells were removed, and adherent cells were cultured in fresh medium containing GM-CSF. On day 6, non-adherent and loosely adherent cells were used in experiments as immature dendritic cells.

**Preparation and Transfection of Octaarginine-Modified Multifunctional Envelope-Type Nano Device (R8-MEND)** The multifunctional envelope-type nano device (MEND) encapsulating protamine-condensed pDNA was prepared by the lipid film hydration method described in a previous reports.[21,22] A stearyl octaarginine (STR-R8) solution (5 mol% of lipids) was added to the suspension of

* To whom correspondence should be addressed. e-mail: kogure@pharm.hokudai.ac.jp

MEND to attach the R8 peptide to the envelope of the MEND, and the mixture was incubated for 30 min at room temperature. R8-MEND containing 0.4 $\mu$g of pDNA suspended in 0.25 ml of DMEM(−) was added to $4\times10^4$ NIH3T3 or HeLa cells, followed by incubation for 3 h at 37 °C. Next, 1 ml of DMEM containing 10% fetal calf serum was added to the cells, followed by a further 45 h incubation. The cells were then washed, and solubilized with reporter lysis buffer (Promega, Madison, WI, U.S.A.). The luciferase reaction was initiated by the addition of 50 $\mu$l of luciferase assay reagent (Promega, Madison, WI, U.S.A.) to 20 $\mu$l of cell lysate, and measured by means of a luminometer (Luminescencer-PSN, ATTO, Japan). The amount of protein in the cell lysate was determined using a BCA protein assay kit (PIERCE, Rockford, IL, U.S.A.). Data are reported as the mean±standard deviation ($n$=3).

**Preparation of NLS-Modified Double Membraneous MEND (NLS-DMEND)** The NLS-modified double membaneous MEND (NLS-DMEND) were prepared by an amended LPD method.[23] First, to prepare NLS-modified small liposomes, lipid film containing unstable lipid DOPE/pH sensitive fusogenic lipid CHEMS (9:2 (molar ratio)) and 1 mol% of stearylated SV40 T antigen-derived NLS (GGP-KKKRKVPKKKRK) was hydrated with 1 ml of 10 mM HEPES buffer (pH 7.4) for 10 min at room temperature. The hydrated lipid film was then sonicated with a probe-type sonicator. Condensed DNA particles were prepared by mixing a DNA solution (0.1 mg/ml) with a protamine solution (0.1 mg/ml) with vortexing at a N/P ratio of 2.2 as mentioned above. The suspensions of NLS-modified small liposomes and condensed DNA were then mixed at a ratio of 2:1 (v/v) to coat the condensed DNA particle by fusion of the NLS-modified small liposomes with a double lipid membrane as reported previously.[23] The final concentrations of lipid and DNA were 0.367 mM and 0.013 mg/ml, respectively.

**Characterization of NLS-DMEND** Hydrodynamic diameter was measured by a quasi-elastic light scattering method by means of an electrophoretic light scattering spectrophotometer (ELS-8000, Otsuka electronics, Japan). A suspension of the NLS-DMEND, which was constructed by a FITC-labeled DNA particle and aqueous rhodamine-entrapped NLS-modified small liposomes, were layered on a discontinuous sucrose density gradient (0 to 30%), and centrifuged at $160000\times\boldsymbol{g}$ for 2 h at 20 °C. A 1 ml aliquot was collected from the top and the fluorescence intensities of FITC and rhodamine were measured. A frozen sample of the double membraneous MEND was observed by cryo transfer observation by transmission electron microscopy (Hitachi H-7650), at a voltage of 120 kV and a magnification of 75000.

**Transfection of NLS-DMEND** A suspension of NLS-DMEND, containing 0.8 $\mu$g of pDNA was added to $2\times10^5$ BMDC, and the suspension incubated for 1 h at 37 °C in 0.2 ml of 10 mM HEPES buffer (pH 6.5) containing 5% glucose to induce fusion of the NLS-DMEND with the plasma membrane. Then, 0.5 ml of RPMI 1640 containing 10% fetal calf serum and 10 ng/ml of GM-CSF was added to the cells, followed by a further 23 h incubation. In the inhibition experiment, BMDC were treated with a mixture of metabolic inhibitors (final concentrations; 1 $\mu$g/ml of Antimycine A, 0.1% (w/v) of $NaN_3$ and 10 mM of NaF) for 30 min at 37 °C before addition of NLS-DMEND. The cells were then washed, and solubilized in reporter lysis buffer. Luciferase activity was measured as mentioned above. Data are reported as the mean±standard deviation ($n$=3). Confocal scanning microscopic analysis of the transfected cells was performed by means of confocal scanning laser microscopy (CLSM) (LSM510 META, Carl Zeiss, Germany) as described previously.[24]

## RESULTS AND DISCUSSION

Nuclear membranes are nearly impenetrable barriers, especially in non-dividing cells, to the nuclear transfer of foreign substances, such as pDNA. In fact, the nuclear transfer of pDNA failed in the transfection of condensed luciferase pDNA coated with lipid, the surface of which was modified with R8 (R8-MEND) (Fig. 1), to non-dividing BMDC, although the R8-MEND showed a significantly high transfection activity in dividing cells (NIH3T3 cells and HeLa cells) by choosing macropinocytosis, which can avoid lysosomal degradation.[25] We then observed the intracellular trafficking of the R8-MEND encapsulating rhodamine-labeled DNA core in the BMDC by CLSM. As shown in Fig. 1c, the DNA of R8-MEND was recognized in BMDC, however, no DNA was observed in nucleus. This result suggests that R8-MEND can not overcome the macropinosomal membrane and/or nuclear membrane of BMDC.

Thus, we designed a NLS-modified MEND to enter directly into cytoplasm by fusion with plasma membrane, and to utilize the NLS/importin system for the nuclear transfer of protamine-condensed pDNA by presenting NLS on the surface of MEND to retain its flexibility. Thus, after internalization by membrane fusion, NLS-modified MEND should be able to approach to nucleus by recognizing the NLS by importin. Therefore, we prepared an NLS-modified double membraneous MEND (NLS-DMEND) consisting of protamine-condensed DNA and pH-sensitive fusogenic lipid membrane to ensure the internalization of the MEND with NLS on the surface into cytoplasm, as shown in Fig. 2a. The diameters and zeta-potential of the condensed DNA particles and NLS-DMEND were 106.3±7.6 nm and 183.4±43.1 nm and 21.4±7.9 mV and −42.7±8.0 mV, respectively. The NLS-DMEND, which was composed of aqueous marker entrapping NLS-modified small liposomes and fluorescent-labeled condensed DNA particle, was subjected to sucrose density gradient fractionation (Fig. 2b). FITC-labeled DNA and rhodamine aqueous marker were coexisted in the same fraction (fraction#11), suggesting that the inner aqueous phase of the liposomes was maintained, even after the coating of condensed DNA particle by the fusion of each liposome. In addition, no fluorescent resonance energy transfer was observed between FITC labeled on DNA and aqueous rhodamine (data not shown). This suggests that the aqueous phase of the liposome and the condensed DNA particles were separated by the lipid envelope. Furthermore, the core structure and surrounding envelope were observed in electron microscopic images (Fig. 2c).

We then observed the intracellular trafficking of NLS-DMEND consisting of rhodamine-labeled DNA (red) and NBD-labeled lipid (green) in the BMDC by CLSM after transfection under mild acidic condition (pH 6.5) to induce direct fusion of only the outermost lipid membrane with the

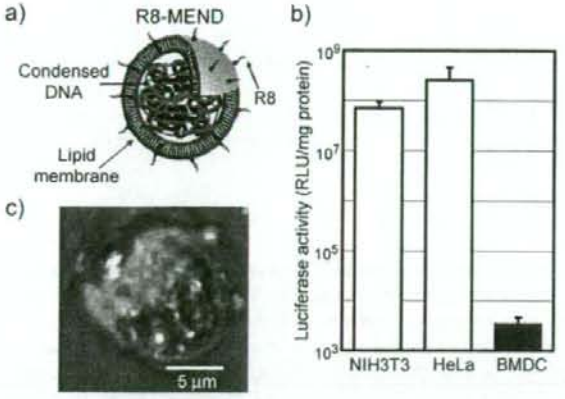


Fig. 1. Schematic Representation, Transfection Activity and Intracellular Trafficking of R8-MEND in BMDC

(a) R8-MEND consists of a protamine-condensed plasmid DNA particle and a lipid membrane. The lipid membrane is modified with the membrane penetrating peptide R8 to improve cellular uptake and intracellular trafficking. (b) Transfection activities of R8-MEND in NIH3T3 cells, HeLa cells and BMDC. (c) Confocal scanning microscopic image of BMDC transfected with R8-MEND encapsulating rhodamine-labeled DNA (red). The nucleus of the BMDC was stained with SYTO24 (green).

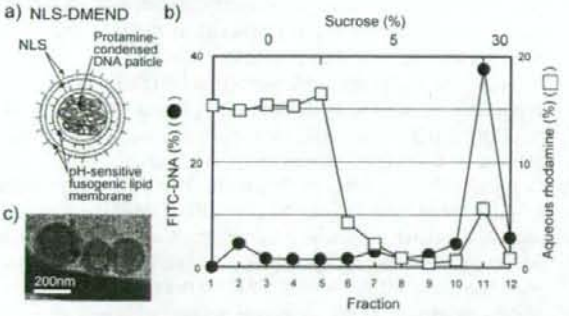


Fig. 2. Schematic Representation and Characterization of NLS-DMEND

(a) Double membranous structure of NLS-DMEND. (b) Distribution of DNA aqueous marker after discontinuous sucrose density gradient fractionation of NLS-DMEND suspension. DNA and aqueous marker were presented by a closed circle (●) and an open square (□), respectively. (c) The DMEND was observed by cryo transmission electron microscopy.

plasma membrane. After the transfection, DNA particles were observed as numerous pink dots in the nucleus (blue) of the BMDC (Fig. 3a). Furthermore, the transfection activity was enhanced by two orders of magnitude compared to R8-MEND (Fig. 3d). However, in the case of normal transfection of NLS-DMEND, no DNA was observed in the BMDC nucleus (Fig. 3b), and luficerase activity was not improved (Fig. 3d). As shown in Fig. 3b, yellow dots indicating the colocalization of DNA and lipid was observed. This suggests that the NLS-DMEND was not able to escape from endosomes after internalization via endocytosis, although membranes of the NLS-DMEND consist of pH-sensitive fusogenic lipids. In addition, we examined the transfection of NLS-modified MEND by direct fusion method to BMDC. However, no transfection activity was detected (data not shown). Probably, the NLS-modified MEND could not present NLS on its surface after internalization, because direct fusion method significantly changed membrane structure of the MEND. These results suggest that condensed pDNA particles were transferred into the nucleus by direct fusion of the NLS-DMEND, and not only NLS peptide but also double-membraneous structure of NLS-DMEND are necessary for transfer of DNA into nucleus of BMDC.

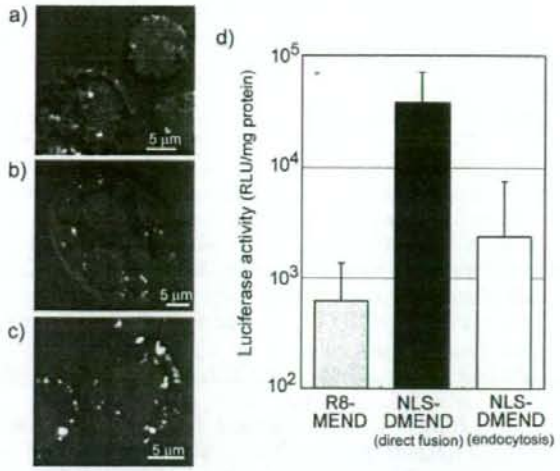


Fig. 3. Intracellular Trafficking of NLS-DMEND after Transfection and Transfection Activities of R8-MEND and NLS-DMEND in BMDC

CLSM images of BMDC transfected with NLS-DMEND by (a) direct fusion and (b) endocytosis. (c) Effect of metabolic inhibitors on intracellular trafficking of NLS-DMEND after trasnfection by direct fusion in BMDC. The NLS-DMEND consists of rhodamine-labeled DNA (red) and NBD-labeled lipid (green). The nucleus was stained with Hoechst (blue). Pink dots denote the colocalization of DNA in the nucleus. (d) Luciferase activities of BMDC transfected with R8-MEND and NLS-DMEND.

We next examined the effect of metabolic inhibitors (Antimycin A, $NaN_3$ and NaF) on the nuclear transfer of condensed DNA by NLS-DMEND. In the presence of metabolic inhibitors, the nuclear transfer of condensed DNA was completely prevented, although no effect was observed on the internalization of the MEND by direct fusion method (Fig. 3c). In addition, no significant luciferase activity was detected after the transfection of NLS-DMEND under this condition (data not shown). Thus, the nuclear transfer of DNA particles was an energy dependent event. It is possible that condensed DNA particles pass, in an energy-dependent manner, through the NPC *via* the nuclear transfer machinery, because we previously clarified the nuclear transfer ability of protamine-condensed pDNA particles by a microinjection technique,[26] and that the protamine-condensed pDNA is highly flexible,[22] although the diameter of the condensed DNA particle (approximately 100 nm) was significantly larger than the NPC pore size.[27,28]

In conclusion, condensed pDNA particles were transferred into the nucleus of non-dividing cells by NLS-DMEND.

**Acknowledgements** This work was supported, in part, by Grants-in-Aid for Scientific Research (B) from the Ministry of Education, Culture, Sports, Science and Technology of Japan, and by Grants-in-Aid for Scientific Research on Priority Areas from the Japan Society for the Promotion of Science. We thank the Hitachi High-Technologies Corporation for generously performing the cryo TEM observation. The authors also with to thank Dr. M. S. Feather for his helpful advice in writing this manuscript.

## REFERENCES


1) Gorlich D., Kutay U., *Annu. Rev. Cell Dev. Biol.*, **15**, 607—660 (1999).
2) Diebold S. S., Kursa M., Wagner E., Cotten M., Zenke M., *J. Biol. Chem.*, **274**, 19087—19094 (1999).
3) Diebold S. S., Plank C., Cotten M., Wagner E., Zenke M., *Somat. Cell Mol. Genet.*, **27**, 65—74 (2002).
4) Mahato R. I., Henry J., Narang A. S., Sabek O., Fraga D., Kotb M., Gaber A. O., *Mol. Ther.*, **7**, 89—100 (2003).
5) Larregina A. T., Morelli A. E., Tkacheva O., Erdos G., Donahue C., Watkins S. C., Thomson A. W., Falo L. D. J., *Blood*, **103**, 811—819 (2004).
6) Laitala-Leinonen T., *J. Negat. Results Biomed.*, **4**, 5—25 (2005).
7) Collas P., Alestrom P., *Mol. Reprod. Dev.*, **45**, 431—438 (1996).
8) Collas P., Alestrom P., *Transgenic Res.*, **7**, 303—309 (1998).
9) Keller M., Harbottle R. P., Perouzel E., Colin M., Shah I., Rahim A., Vaysse L., Bergau A., Moritz S., Brahimi-Horn C., Coutelle C., Miller A. D., *Chembiochem*, **4**, 286—298 (2003).
10) Akita H., Tanimoto M., Masuda T., Kogure K., Hama S., Ninomiya K., Futaki S., Harashima H., *J. Gene Med.*, **8**, 198—206 (2005).
11) Sebestyen M. G., Ludtke J. J., Bassik M. C., Zhang G., Budker V., Lukhtanov E. A., Hagstrom J. E., Wolff J. A., *Nat. Biotechnol.*, **16**, 80—85 (1998).
12) Ciolina C., Byk G., Blanche F., Thuillier V., Scherman D., Wils P., *Bioconjug. Chem.*, **10**, 49—55 (1999).
13) Neves C., Byk G., Scherman D., Wils P., *FEBS Lett.*, **453**, 41—45 (1999).
14) Zanta M. A., Belguise-Valladier P., Behr J. P., *Proc. Natl. Acad. Sci. U.S.A.*, **96**, 91—96 (1999).
15) Escriou V., Carriere M., Scherman D., Wils P., *Adv. Drug Deliv. Rev.*, **55**, 295—306 (2003).
16) van der Aa M. A., Koning G. A., d'Oliveira C., Oosting R. S., Wilschut K. J., Hennink W. E., Crommelin D. J., *J. Gene Med.*, **7**, 208—217 (2005).
17) Tanimoto M., Kamiya H., Minakawa N., Matsuda A., Harashima H., *Bioconjug. Chem.*, **14**, 1197—1202 (2003).
18) Futaki S., Ohashi W., Suzuki T., Niwa M., Tanaka S., Ueda K., Harashima H., Sugiura Y., *Bioconjug. Chem.*, **12**, 1005—1011 (2001).
19) Inaba K., Pack M., Inaba M., Sakuta H., Isdell F., Steinman R. M., *J. Exp. Med.*, **186**, 665—672 (1997).
20) Akazawa T., Masuda H., Saeki Y., Matsumoto M., Takeda K., Tsujimura K., Kuzushima K., Takahashi T., Azuma I., Akira S., Toyoshima K., Seya T., *Cancer Res.*, **64**, 757—764 (2004).
21) Kogure K., Moriguchi R., Sasaki K., Ueno M., Futaki S., Harashima H., *J. Control. Release*, **98**, 317—323 (2004).
22) Moriguchi R., Kogure K., Akita H., Futaki S., Miyagishi M., Taira K., Harashima H., *Int. J. Pharm.*, **301**, 277—285 (2005).
23) Lee R. J., Huang L., *J. Biol. Chem.*, **271**, 8481—8487 (1996).
24) Akita H., Ito R., Khalil I. A., Futaki S., Harashima H., *Mol. Ther.*, **9**, 443—451 (2004).
25) Khalil I. A., Kogure K., Futaki S., Harashima H., *J. Biol. Chem.*, **281**, 3544—3551 (2006).
26) Masuda T., Akita H., Harashima H., *FEBS Lett.*, **579**, 2143—2148 (2005).
27) Pante N., Kann M., *Mol. Biol. Cell.*, **13**, 425—434 (2002).
28) Akuta T., Eguchi A., Okuyama H., Senda T., Inokuchi H., Suzuki Y., Nagoshi E., Mizuguchi H., Hayakawa T., Takeda K., Hasegawa M., Nakanishi M., *Biochem. Biophys. Res. Commun.*, **297**, 779—786 (2002).

JPP Journal of Pharmacy and Pharmacology

JPP 2006, 58: 431–437
© 2006 The Authors
Received August 9, 2005
Accepted December 20, 2005
DOI 10.1211/jpp.58.4.0002
ISSN 0022-3573

Graduate School of Pharmaceutical Sciences, Hokkaido University, Kita-12, Nishi-6, Kita-ku, Sapporo 060-0812, Japan

Yoshio Nakamura, Kentaro Kogure, Yuma Yamada, Hideyoshi Harashima

CREST Japan Science and Technology Agency (JST), Japan

Kentaro Kogure, Hideyoshi Harashima

PRESTO Japan Science and Technology Agency (JST), Japan

Shiroh Futaki

Institute for Chemical Research, Kyoto University, Uji, Kyoto 611-0011, Japan

Shiroh Futaki

**Correspondence:** K. Kogure, Graduate School of Pharmaceutical Sciences, Hokkaido University, Kita 12, Nishi 6, Kita-ku, Sapporo 060-0812, Japan. E-mail: kogure@pharm.hokudai.ac.jp

**Funding:** This work was supported, in part, by Grants-in-Aid for Scientific Research (B) from the Ministry of Education, Culture, Sports, Science and Technology of Japan, and by Grants-in-Aid for Scientific Research on Priority Areas from the Japan Society for the Promotion of Science.



# Significant and prolonged antisense effect of a multifunctional envelope-type nano device encapsulating antisense oligodeoxynucleotide

Yoshio Nakamura, Kentaro Kogure, Yuma Yamada, Shiroh Futaki and Hideyoshi Harashima

## Abstract

A multifunctional envelope-type nano device (MEND) was developed for use as an efficient non-viral system for the delivery of plasmid DNA (pDNA) using octaarginine (R8) as an internalizing ligand. Three types of R8-MENDs were prepared, co-encapsulating luciferase-encoding pDNA and anti-luciferase oligodeoxynucleotide (ODN) condensed by three polycations, stearyl octaarginine (STR-R8), poly-L-lysine (PLL) and protamine, and the antisense effects of the ODN-encapsulated R8-MENDs (ODN-MEND) were analysed in-vitro. The ODN-MEND packaged using protamine as a condenser showed a 90% antisense effect 16 h after the transfection, and a persistent antisense effect of over 75% for up to 48 h, which was much more effective than that of LipofectAmine2000. On the other hand, the ODN-MENDs prepared using PLL and STR-R8 as condensers did not show any significant inhibition of luciferase activity. Although there was no specific relation between the physicochemical characteristics of the ODN-MENDs and their antisense effect, the pattern of the antisense effect among the ODN-MENDs was similar to that of the silencing effect of R8-MEND encapsulating plasmid DNA encoding siRNA. These results suggest that R8-MENDs are able to deliver encapsulated DNA to the cytosol as well as to the nucleus, and that protamine can also function as an efficient decondenser, not only in the nucleus but also in the cytosol. In conclusion, we successfully developed an ODN-MEND with a high antisense effect using protamine as a DNA condensing as well as a decondensing agent.

## Introduction

In the field of gene silencing research, the use of antisense oligodeoxynucleotides (ODNs) has various advantages, such as their ability to target introns and modification for the improvement of selectivity and efficacy (Scherer & Rossi 2003). Zamecnik & Stephenson first demonstrated that a 13-mer ODN complementary to terminally repeated sequences in the long terminal repeat of the Rous sarcoma virus (RSV) inhibited RSV translation in a cell-free system and viral replication in cultured cells (Stephenson & Zamecnik 1978; Zamecnik & Stephenson 1978). Since then, attempts have been made to use ODN-based approaches therapeutically in treating serious diseases, such as cancer (Miyake et al 2001) and hypertension (Phillips 2001). However, there are some problems associated with this approach, such as degradation by nucleases and difficulties associated with targeting and intracellular delivery (Shi & Hoekstra 2004). Thus, an efficient method of packaging ODNs is needed to solve these problems.

Several packaging methods for an ODN have already been reported. Gokhale et al (1997) encapsulated ODN with a lipid membrane by rehydrating a dried lipid film in the presence of ODN. Shi & Hoekstra (2004) reported on the encapsulation of an ODN with a cationic lipid by a freeze–thaw method. In addition, Semple et al (2001) constructed stabilized antisense-lipid particles (SALP) by packaging an ODN with a pH-sensitive cationic lipid. These methods were based on electrostatic interactions

between the anionic ODN and the cationic lipids. Each method, however, required a lengthy procedure and the encapsulation efficiency was low.

We developed a multifunctional envelope-type nano device (MEND) as a novel delivery system of plasmid DNA (pDNA) (Kogure et al 2004). MEND is a liposomal-type non-viral delivery system that mimics an envelope-type virus, and is composed of a positively charged condensed DNA core covered with a negatively charged lipid membrane based on electrostatic interactions. Furthermore, the MEND can be equipped with various functional devices, such as a pH-sensitive fusogenic peptide for membrane fusion (Yamada et al 2005a), a ligand for specific targeting (Kakudo et al 2004), a cell-penetrating peptide for efficient cellular uptake and polyethylenglycol for stabilization in the circulating blood by controlling the topology of the envelope membrane (Sasaki et al 2005). Using this system, the transfection activity of the MEND was enhanced by two orders of magnitude by introducing stearyl octaarginine (STR-R8), a well-known and efficient cell-penetrating peptide (Futaki et al 2001; Nakase et al 2004), on the envelope (Kogure et al 2004).

We recently also developed a novel packaging method for an ODN to a MEND (Yamada et al 2005b). The encapsulation efficiency and preparation time for this method were significantly better than those of the SALP method and the freeze–thaw method. In this study, we report on the construction of three types of octaarginine-modified MEND (R8-MEND) encapsulating ODN condensed by three polycations (STR-R8, poly-L-lysine (PLL) and protamine) and then compared the antisense effects of the ODN-encapsulated R8-MENDs.

## Material and Methods

### Materials

1,2-Dioleoyl-sn-glycero-3-phosphoethanolamine (DOPE) was purchased from AVANTI Polar Lipids Inc. (Alabaster, AL, USA). Cholesteryl hemisuccinate (5-cholesten-3-ol 3-hemisuccinate; CHEMS) and poly-L-lysine (PLL; MW 27 400) were obtained from Sigma-Aldrich Co. (St Louis, MO, USA). Stearyl octaarginine (STR-R8) was synthesized as described previously (Futaki et al 2001). Protamine sulfate was purchased from Merck KGaA (Darmstadt, Germany). LipofectAmine 2000 was obtained from Invitrogen Co. (Carlsbad, CA, USA). The pDNA pCMV-luc (7037 bp) encoding luciferase was prepared by EndFree Plasmid Mega Kit (Qiagen GmbH, Hilden, Germany). The anti-luciferase antisense ODN (19mer, 5′-AACCGCTTCCCC GACTTCC-3′) used a sequence reported (Xu et al 2003), and was obtained from Sigma-Aldrich Japan K.K. (Tokyo, Japan). NIH3T3 cells were obtained from the American Type Culture Collection (Manassas, VA, USA).

### Preparation of R8-MEND

The procedure for the preparation of R8-MEND comprised four steps as follows (schematically shown in Figure 1) (Kogure et al 2004).

Firstly, for DNA (ODN or pDNA) condensation with a polycation (PLL, STR-R8, and protamine), DNA and the polycation were dissolved with 10 mM HEPES buffer (pH 7.4). To condense the DNA, the DNA solution ($0.1\,mg\,mL^{-1}$) was added to the polycation solution ($0.1\,mg\,mL^{-1}$) under vortexing at room temperature. In

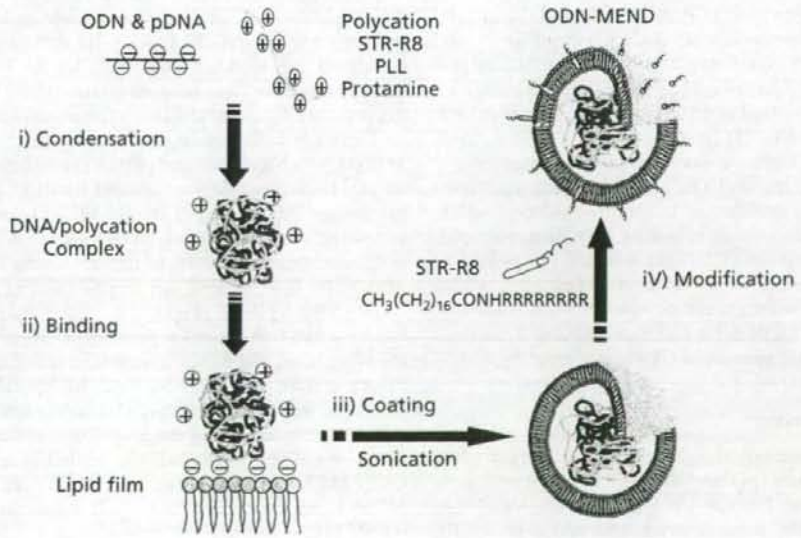


**Figure 1** Scheme for the packaging of the ODN-MEND. The packaging comprised 4 steps: i, condensation of ODN; ii, binding of condensed-ODN to lipid film; iii, lipid coating by sonication; iv, modification of the lipid membrane by STR-R8.

the case of co-packaging of ODN and pDNA to the MEND, the weight ratio of ODN to pDNA was 1:1 (748:1 mol/mol). The DNA content of a suspension of the DNA/STR-R8 complex prepared at a nitrogen/phosphate (N/P) ratio of 2.9 was 0.033 mg $mL^{-1}$. The DNA content of a suspension of the DNA/PLL complex prepared at a nitrogen/phosphate (N/P) ratio of 2.4 was 0.05 mg $mL^{-1}$. The DNA content of suspension of DNA/protamine complex prepared at a nitrogen/phosphate (N/P) ratio of 2.2 was 0.04 mg $mL^{-1}$.

Secondly, electrostatic binding of condensed DNA to lipid film was carried out. After the condensation of DNA, 0.25 mL of the DNA/polycation complex (DPC) suspension was added to the lipid film, formed by the evaporation of a chloroform solution of 137.5 nmol lipids (DOPE/CHEMS = 9:2 (molar ratio)) on the bottom of a glass tube, followed by incubation for 10 min to hydrate the lipids. The final concentration of lipid was 0.55 mM.

Thirdly, the condensed DNA was coated with lipid. To coat the DPC with lipids, the glass tube was sonicated for about 1 min in a bath-type sonicator (125 W, Branson Ultrasonics, Danbury, CT, USA).

Finally, modification of the lipid envelope with R8 peptide was carried out. An STR-R8 solution (5 mol% of lipids) was added to the suspension to attach the membrane-permeable peptide R8 to the envelope of the lipid-coated particle, and the mixture was then incubated for 30 min at room temperature.

The hydrodynamic diameter was measured by a quasi-elastic light-scattering method and the zeta-potential was determined electrophoretically by means of an electrophoretic light-scattering spectrophotometer (ELS-8000, Otsuka Electronics, Japan).

### Sucrose density gradient fractionation

R8-MEND containing FITC-labelled ODN (15% of total ODN) and rhodamine-labelled DOPE (1 mol% of total lipids) was layered on a discontinuous sucrose density gradient (0–60%), and centrifuged at 160 000 *g* for 2 h at 20°C. A 1-mL sample was collected from the top and the fluorescence intensities of FITC and rhodamine were measured. Furthermore, to estimate fluorescence resonance energy transfer (FRET) between FITC and rhodamine, each fraction sample was solubilized in 1% sodium dodecyl sulfate (SDS), and the fluorescence intensities were then measured. The trapped amount of ODN was obtained by the sum of fluorescent intensities of FITC in the fractions, which showed FRET. The encapsulation efficiency was calculated by the amount of ODN in the ODN-encapsulated fractions divided by the total amount of ODN multiplied by 100.

### Co-transfection assay

The MEND containing 0.04 $\mu$g DNA (pDNA:ODN = 1:748, mol:mol) or lipoplex (pDNA:ODN = 1:748, mol:mol) containing 0.04 $\mu$g with LipofectAmine2000 were suspended in 0.25 mL of DMEM without serum and added to $4 \times 10^4$ NIH3T3 cells followed by incubation for 3 h at 37°C. Next, 1 mL of DMEM containing 10% fetal calf serum was added to the cells, followed by a further incubation for 5, 13, 21 or 45 h. The cells were then washed, and solubilized with reporter lysis buffer (Promega, Madison, WI). Luciferase activity was initiated by the addition of 100 $\mu$L of luciferase assay reagent (Promega) to 20 $\mu$L of cell lysate, and measured by means of a luminometer (Luminescencer-PSN; ATTO, Japan). The amount of protein in the cell lysate was determined using a BCA protein assay kit (PIERCE, Rockford, IL, USA). The control luciferase activity was determined using control MEND encapsulating luciferase pDNA and anti-green fluorescent protein (GFP) ODN as non-related control ODN. The percentage of antisense effect was calculated by subtracting the luciferase activity of the ODN-encapsulated R8-MEND (antisense) from the control luciferase activity divided by the control luciferase activity multiplied by 100.

### Statistical analysis

Statistical analysis of the effect of the formulation on various physicochemical properties was performed using a one-way analysis of variance and Tukey's test. The effect of formulation type and time on the antisense effect was evaluated using a repeated measures analysis of variance and Tukey's test. $P < 0.05$ denoted significance in all cases.

## Results and Discussion

We recently reported on the successful packaging of an antisense ODN in a MEND by the lipid hydration method (Yamada et al 2005b). The R8-MEND encapsulating ODN (ODN-MEND) would be expected to exhibit a significant antisense effect, since an R8-MEND encapsulating an siRNA expression plasmid showed a potent silencing effect in-vitro (Moriguchi et al 2005). In the siRNA experiment, we prepared three R8-MENDs, in which plasmid DNA had been condensed using three different polycations (PLL, STR-R8 and protamine) and compared the silencing effects of the R8-MENDs. The most potent effect was induced by the MEND encapsulating protamine-condensed DNA (Moriguchi et al 2005).

Therefore, in this study, we prepared three types of ODN-MEND, which encapsulated pDNA encoding luciferase and an anti-luciferase ODN condensed by PLL, STR-R8 and protamine. Preparation of the R8-MEND consists of four steps (i.e., condensation of ODN or pDNA with polycations, electrostatic binding of the condensed DNA to lipid membrane, lipid coating and modification of the envelope surface with STR-R8 (Figure 1)). In this study, DNA was condensed by polycations as positively charged particles. On the other hand, the MEND showed negative zeta-potential before surface modification with R8 peptide (data not shown). These results indicate that condensed DNA particles were trapped inside the MENDs in all three preparations. We then examined the antisense effect of the ODN-MENDs by transfecting NIH3T3 cells. The R8-MEND encapsulating the STR-R8-condensed ODN (ODN-MEND(STR-R8)) showed a low silencing effect (15%) 8 h after transfection, and no silencing effect was observed at 24 h (Table 1). The R8-MEND encapsulating

**Table 1** Antisense effect of ODN-MEND(STR-R8), ODN-MEND(PLL) and ODN-MEND(Prot) encapsulating luciferase-pDNA and anti-luciferase antisense ODN in NIH3T3 cells

| | Antisense effect (%) | | | |
|---|---|---|---|---|
| | 8 h | 16 h | 24 h | 48 h |
| OND-MEND(PLL) | 0 ± 0 | 0 ± 0 | 0 ± 0 | 0 ± 0 |
| ODN-MEND(STR-R8) | 15.2 ± 25.6 | 13.0 ± 22.6 | 0 ± 0 | 3.7 ± 6.5 |
| ODN-MEND(Prot) | 71.7 ± 9.3 | 93.4 ± 3.2 | 85.7 ± 6.6 | 77.6 ± 16.3 |
| Lipofectamine2000 | 54.8 ± 21.0 | 46.0 ± 22.0 | 27.6 ± 3.6 | 13.4 ± 10.7 |

Luciferase activity was measured at 8, 16, 24 and 48 h after the transfection of NIH3T3 cells with the ODN-MEND. The percentage of the antisense effect was calculated by subtracting the luciferase activity of ODN-MEND (antisense) from the control luciferase activity divided by control luciferase activity multiplied by 100. The values are the means ± s.d., n = 3.

PLL-condensed ODN (ODN-MEND(PLL)) did not show any silencing effect. The R8-MEND encapsulating the protamine-condensed ODN (ODN-MEND(Prot)), however, significantly inhibited luciferase activity (i.e., the silencing effect of ODN-MEND(Prot) was 90% at 16 h after transfection, and was maintained at 77% for periods of up to 48 h). There were significant differences among the formulations, except for between ODN-MEND(PLL) and ODN-MEND(STR-R8). However, no significant difference was observed in the effect of incubation time on the antisense effects. This pattern of the antisense effect among ODN-MENDs was similar to those of R8-MENDs encapsulating plasmid DNA encoding siRNA (Moriguchi et al 2005), although the physicochemical characteristics of ODNs are significantly different from plasmid DNA. On the other hand, the silencing effect of LipofectAmine 2000 (LA2000), a commercially available transfection reagent, was only 55% at 8 h after the co-transfection of luciferase-pDNA and anti-luciferase ODN, and this decreased to 13% at 48 h (Table 1). ODN-MEND(Prot) and LA2000 showed significant toxicity (Table 2). However, no toxicity was observed in ODN-MEND(PLL)- and ODN-MEND(STRR8)-treated cells. In addition, protamine should have little toxicity, because that peptide is approved by the FDA for clinical use in the USA (Sorgi et al 1997). This therefore suggests that the antisense effect of ODN-MEND(Prot) is related to its toxicity. On the other hand, LA2000 seems to have inherent toxicity by itself, because the toxicity of LA2000 was higher than that of ODN-MEND(Prot), although the difference was not significant.

The cellular up-take of the MENDs is suggested to be almost the same, because all the MENDs were coated with the same lipid membrane, and there was no significant difference in their zeta-potentials (Table 3). Thus, it is suggested that uptake efficiency is not responsible for the difference in antisense effects of the MENDs. Then, we compared the transfection activity of the three MENDs, since the inhibitory effects of ODN-MENDs were expected to be influenced by transfection efficiency of pDNA. As summarized in Table 4, no significant difference was observed in the luciferase activity of the three types of MENDs in NIH3T3 cells. In our previous report, however, R8-MEND(Prot) showed a higher activity than the other MENDs in COS7 cells. This discrepancy is likely due to differences in experimental conditions, such as the cell type and amount of pDNA. Therefore, it is suggested that transfection efficiency did not affect the antisense effects of ODN-MENDs in the present experimental conditions.

We then performed a sucrose density gradient fractionation to compare the morphological characteristics, such

**Table 2** Comparison of the toxicity of ODN-MENDs with LA2000

| Treatment | MTT assay values (%) |
|---|---|
| ODN-MEND(PLL) | 100.0 ± 13.5 |
| ODN-MEND(STR-R8) | 79.6 ± 10.0 |
| ODN-MEND(Prot) | 58.8 ± 6.5 |
| LA2000 | 40.3 ± 5.3 |

The toxicity of ODN-MENDs and LA2000 was evaluated by MTT assay of the cells 48 h after the transfection with them. Values of MTT assay were represented by percentage of absorbance of the transfected cells divided by that of non-treatment cells multiplied by 100. The ODN-MEND(Prot) and LA2000 showed significant toxicity as compared with non-treatment ($P < 0.05$). The values are the means ± s.d., n = 3.

**Table 3** Characteristics of ODN-MEND(STR-R8), ODN-MEND(PLL) and ODN-MEND(Prot)

| ODN-MEND | Diameter (nm) | Zeta-potential (mV) | Encapsulation efficiency (%) |
|---|---|---|---|
| STR-R8 | 377 ± 7 | 46.9 ± 5.6 | 91.3 ± 1.3 |
| PLL | 389 ± 7 | 39.6 ± 5.6 | 90.2 ± 3.2 |
| Protamine | 397 ± 5 | 40.4 ± 9.4 | 92.4 ± 2.1 |

The encapsulation efficiency was calculated by the amount of ODN in ODN encapsulated fractions divided by the total amount of ODN multiplied by 100. A significant difference was observed only between the diameters of STR-R8 and protamine ($P < 0.05$). The values are the means ± s.d., n = 3.

**Table 4** Comparison of transfection activity of ODN-MENDs at various incubation periods

| | Luciferase activity (RLU (mg protein)$^{-1}$) | | | |
|---|---|---|---|---|
| | 8 h | 16 h | 24 h | 48 h |
| OND-MEND(PLL) | $4.7 \times 10^3 \pm 3.4 \times 10^3$ | $1.2 \times 10^4 \pm 1.4 \times 10^4$ | $2.5 \times 10^4 \pm 9.2 \times 10^3$ | $1.2 \times 10^5 \pm 1.7 \times 10^5$ |
| ODN-MEND(STR-R8) | $1.1 \times 10^4 \pm 6.3 \times 10^3$ | $9.4 \times 10^4 \pm 8.2 \times 10^4$ | $3.7 \times 10^5 \pm 3.4 \times 10^5$ | $1.1 \times 10^6 \pm 4.2 \times 10^5$ |
| ODN-MEND(Prot) | $4.3 \times 10^4 \pm 3.5 \times 10^4$ | $9.1 \times 10^4 \pm 6.2 \times 10^4$ | $4.8 \times 10^5 \pm 4.0 \times 10^5$ | $4.8 \times 10^5 \pm 2.6 \times 10^5$ |

Luciferase activity was measured at 8, 16, 24 and 48 h after the transfection of NIH3T3 cells with the ODN-MEND. No significant difference was observed among the three types of MENDs. The values are the means ± s.d., n = 3.

as density and ratio of ODN to lipid, among the three types of ODN-MENDs, because the difference in morphological characteristics was expected to relate to the function of the ODN-MEND. In the case of ODN-MEND(STR-R8), the ODN was distributed heterogeneously in fractions no. 4 (10–15%), 7 (20–25%), 9(25–30%) and 10 (30–40%) (Figure 2A), indicating the structural heterogeneity of the ODN-MEND(STR-R8). On the other hand, sucrose density gradient fractionation of ODN-MEND(PLL) and ODN-MEND(Prot) showed a homogenous distribution of the MENDs (Figures 2B and 2C). Most of the ODN was detected in fractions no. 10 (30–40%) and 11 (40–60%) in the cases of ODN-MEND(PLL) and ODN-MEND(Prot). Both ODN-MENDs had a higher density and a more homogenous distribution than the ODN-MEND(STR-R8). The size and zeta-potential of the ODN-MENDs are summarized in Table 3. The diameters of all of the ODN-MENDs were around 380 nm, and the zeta-potentials were significantly positive. The diameter of ODN-MEND(Prot) was slightly, but significantly, larger than that of ODN-MEND(STR-R8). However, there was no significant difference among the zeta-potentials of any of the ODN-MENDs. In addition, the successful packaging of all the ODN-MENDs was shown by the co-existence of lipid and ODN, and the elimination of the fluorescent resonance energy transfer (FRET) between rhodamine-labelled lipid and an FITC-labelled ODN with SDS (data not shown). The encapsulation efficiency of the three ODN-MENDs was over 90%. Only ODN-MEND(Prot), however, showed a significant antisense effect (Table 1). This suggests that there is no relation between the physicochemical characteristics of the ODN-MENDs and their antisense effects.

Thus, the condensation state of the ODN appears to be responsible for the difference in antisense effect of the three types of ODN-MENDs, since the effects were dependent on polycations. Furthermore, these findings suggest that a relationship between the condensation state of DNA and the function of the R8-MEND exists, because the electrophoretic pattern of the plasmid DNA encapsulated in R8-MEND with protamine, which showed the highest silencing effect, was different from those prepared using PLL and STR-R8 (Moriguchi et al 2005). We then measured the diameter and zeta-potential of ODNs condensed using PLL, STR-R8 and protamine at various nitrogen/phosphate (N/P) ratios to compare the condensing state of the ODN with the three polycations (Figure 3). In the case of PLL, the diameter was less than 100 nm and the zeta-potential was positive (about 10–20 mV) above an N/P ratio of 2.4. Aggregation was observed at an N/P ratio of 1.8, where the zeta-potential was neutral. The condensed ODN had a diameter of about 130–170 nm and was negatively charged (−20 to −30 mV) below the neutral point. Similarly, in the case of STR-R8, aggregation was also observed at an N/P ratio of 1.2, and the diameter and zeta-potential patterns were similar to samples prepared using PLL. On the other hand, in the case of protamine, no aggregation was observed, and the diameters were in the range 100–200 nm, although the zeta-potential pattern was similar to the others. A significant difference was observed between the diameters of ODN particles condensed by PLL and protamine or STR-R8 and protamine at N/P = 2.4. On the other hand, no significant difference was observed among zeta-potentials.

PLL and STR-R8 are homopolymers of positively charged amino acids, while protamine (amino-acid sequence: PRRRRSSSRPVRRRRRPRVSRRRRRRGGRRRR) consists of 4 oligo-arginine regions separated by several neutral amino acids. The size of the protamine-condensed particles was larger than that of the PLL- and STR-R8-condensed particles as shown in Figure 3A. In addition, we previously reported that the protamine-condensed pDNA core of the MEND was more flexible than PLL- and STR-R8-condensed cores (Moriguchi et al 2005). These observations suggest that a protamine-condensed DNA core is more easily decondensed than PLL and STR-R8, because the non-charged amino acids in the protamine sequence could prevent tight interactions between the DNA and oligo-arginine regions. Another possibility is that the morphological characteristics, such as particle size and zeta-potential, at different N/P ratios, relate to the difference in decondensability of condensed DNA core. In fact, the size and zeta-potential of the core particle condensed with protamine (N/P = 2.2) were larger than those with PLL (N/P = 2.4) and STR-R8 (N/P = 2.9) (Figure 3). However, the decondensability of pDNA in all MENDs appeared to be almost the same under the present experimental conditions, because there was no significant difference among the gene expression of all MENDs (Table 4). This therefore suggests that the decondensation of ODN is different in the three types of

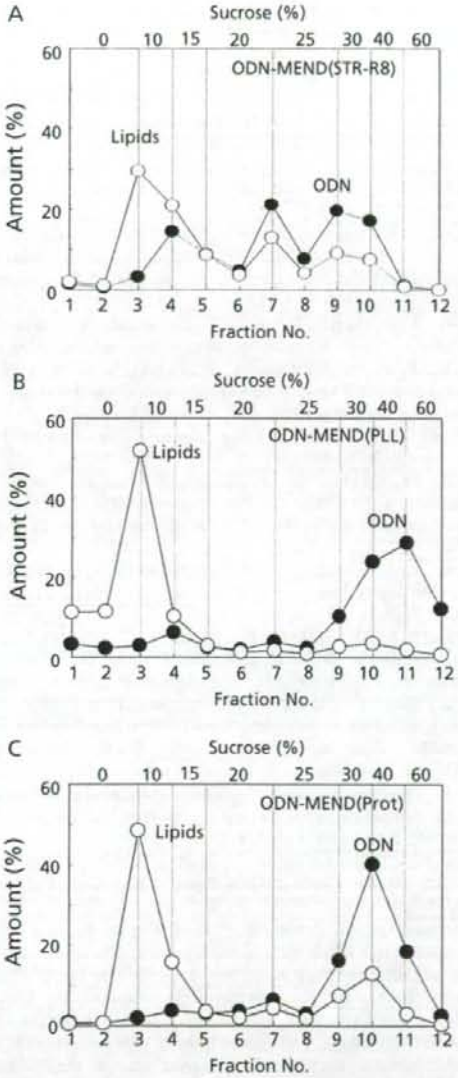


**Figure 2** Distribution of ODN and lipids after discontinuous sucrose density gradient ultracentrifugation of the ODN-MEND. A. ODN-MEND(STR-R8). B. ODN-MEND(PLL). C. ODN-MEND(Prot). Amounts of ODN (●) and lipids (○) were estimated by measuring the fluorescence intensity of FITC-labelled ODN and rhodamine-labelled lipid in each fraction, respectively, n = 2.

MENDs, since the antisense effect was dependent on the polycation used (i.e. ODN-MEND(Prot) showed the most potent antisense effect (Table 1)). This discrepancy between pDNA and ODN should be due to the unique characteristics of ODN, such as its very short length and single-stranded structure. Thus, the protamine-condensed DNA is probably delivered to the cytosol and ODN is released efficiently from the protamine-condensed particle.

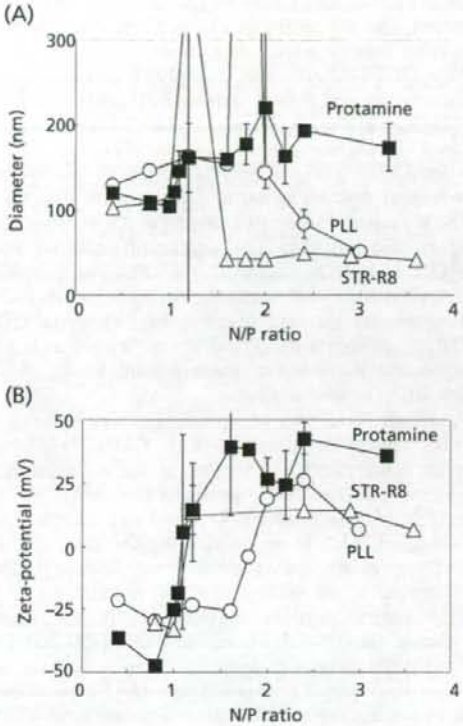


**Figure 3** Relationship between N/P ratio and the diameter or zeta-potential of the ODN condensed with polycations. An ODN solution was added to a polycation solution, such as STR-R8 (△), PLL (○) or protamine (■), under vortexing at room temperature and the diameter (A) and zeta-potential (B) were then measured. At N/P = 2.4, a significant difference was observed between diameters of ODN particles condensed by PLL and protamine or STR-R8 and protamine, n = 3.

On the other hand, it has previously been reported that the protamine-condensed plasmid DNA of R8-MEND could be decondensed efficiently after delivery to the nucleus (Moriguchi et al 2005). Actually, we recently demonstrated by means of a nuclear microinjection technique that the intranuclear transcription efficiency of protamine/DNA complex was significantly higher than that of the PLL/DNA complex (Masuda et al 2005). In addition, it is possible that the R8 peptide assists not only the internalization of MENDs into cells but also the nuclear transfer of pDNA. This suggests that R8-MENDs are able to deliver encapsulated DNA to the cytosol as well as the nucleus, and that protamine plays a role as an efficient decondenser of the condensed DNA core of the R8-MEND, not only in the nucleus but also in the cytosol.

## Conclusions

Three types of R8-MENDs co-encapsulating luciferase-encoding pDNA and anti-luciferase ODN condensed by

three polycations, STR-R8, PLL and protamine, were prepared, and the antisense effects of the ODN-MENDs on luciferase activity were determined.

The ODN-MEND packaged using protamine as a condenser showed a 90% antisense effect 16 h after the transfection, and a persistent antisense effect of over 75% up to 48 h. On the other hand, the silencing effect of LipofectAmine 2000 was only 55% 8 h after the co-transfection, and this decreased to 13% at 48 h. The ODN-MENDs prepared using PLL and STR-R8 as condensers, however, did not show any significant antisense effect. The ODN-MENDs packaged with PLL or protamine were high density and homogeneous as demonstrated by sucrose density gradient fractionation, while the ODN-MEND packaged with STR-R8 was heterogeneous. In addition, the diameters and zeta-potentials of the three ODN-MENDs were similar.

Although there was no specific relation between the physicochemical characteristics of the ODN-MENDs and their antisense effect, the pattern of the antisense effect among the ODN-MENDs was similar to those of the silencing effect of the R8-MEND encapsulating plasmid DNA encoding siRNA. These results suggest that the R8-MENDs are able to deliver encapsulated DNA to the cytosol as well as to the nucleus, and that protamine can also function as an efficient decondenser not only in the nucleus but also in the cytosol. Collectively, ODN-MEND(Prot) with a significant and prolonged antisense effect was successfully developed. This type of ODN-MEND promises to serve as a useful tool in gene silencing research.

## References


Brewer, L. R., Corzett, M., Balhorn, R. (1999) Protamine-induced condensation and decondensation of the same DNA molecule. *Science* **286**: 120–123

Futaki, S., Ohashi, W., Suzuki, T., Niwa, M., Tanaka, S., Ueda, K., Harashima H., Sugiura, Y. (2001) Stearylated arginine-rich peptides: a new class of transfection system. *Bioconjug. Chem.* **12**: 1005–1011

Gokhale, P. C., Soldatenkov, V., Wang, F. H., Rahman, A., Dritschilo, A., Kasid, U. (1997) Antisense raf oligodeoxyribonucleotide is protected by liposomal encapsulation and inhibits Raf-1 protein expression in vitro and in vivo: implication for gene therapy of radioresistant cancer. *Gene Ther.* **4**: 1289–1299

Kakudo, T., Chaki, S., Futaki, S., Nakase, K. I., Akaji, K., Kawakami, T., Maruyama, K., Kamiya, H., Harashima, H. (2004) Transferrin-modified liposomes equipped with a pH-sensitive fusogenic peptide: an artificial viral-like delivery system. *Biochemistry* **18**: 5618–5628

Khalil, I. A., Futaki, S., Niwa, M., Baba, Y., Kaji, N., Kamiya, H., Harashima, H. (2004) Mechanism of improved gene transfer by the N-terminal stearylation of octaarginine: enhanced cellular association by hydrophobic core formation. *Gene Ther.* **11**: 636–644

Kogure, K., Moriguchi, R., Sasaki, K., Ueno, M., Futaki, S., Harashima, H. (2004) Development of a non-viral multifunctional envelope-type nano device by a novel lipid film hydration method. *J. Control. Release* **98**: 317–323

Masuda, T., Akita, H., Harashima, H. (2005) Evaluation of nuclear transfer and transcription of plasmid DNA condensed with protamine by microinjection: the use of a nuclear transfer score. *FEBS Lett.* **579**: 2143–2148

Miyake, H., Hara, I., Kamidono, S., Gleave, M. (2001) Novel therapeutic strategy for advanced prostate cancer using antisense oligodeoxynucleotides targeting anti-apoptotic genes upregulated after androgen withdrawal to delay androgen-independent progression and enhance chemosensitivity. *Int. J. Urol.* **8**: 337–349

Moriguchi, R., Kogure, K., Akita, H., Futaki, S., Miyagishi, M., Taira, K., Harashima, H. (2005) A multifunctional envelope-type nano device for novel gene delivery of siRNA plasmids. *Int. J. Pharm.* **301**: 277–285

Nakase, I., Niwa, M., Takeuchi, T., Sonomura, K., Kawabata, N., Koike, Y., Takehashi, M., Tanaka, S., Ueda, K., Simpson, J. C., Jones, A. T., Sugiura, Y., Futaki, S. (2004) Cellular uptake of arginine-rich peptides: roles for macropinocytosis and actin rearrangement. *Mol. Ther.* **10**: 1011–1022

Phillips, M. I. (2001) Gene therapy for hypertension. *Hypertension* **38**: 543–548

Sasaki, K., Kogure, K., Chaki, S., Kihira, Y., Ueno, M., Harashima, H. (2005) Construction of multifunctional envelope-type nano device by a SUV*-fusion method. *Int. J. Pharm.* **296**: 142–150

Scherer, L. J., Rossi, J. J. (2003) Approaches for the sequence-specific knockdown of mRNA. *Nat. Biotechnol.* **21**: 1457–1465

Semple, S. C., Klimuk, S. K., Harasym, T. O., Dos Santos, N., Ansell, S. M., Wong, K. F., Maurer, N., Stark, H., Cullis, P. R., Hope, M. J., Scherrer, P. (2001) Efficient encapsulation of antisense oligonucleotides in lipid vesicles using ionizable aminolipids: formation of novel small multilamellar vesicle structures. *Biochim. Biophys. Acta* **1510**: 152–166

Shi, F., Hoekstra, D. (2004) Effective intracellular delivery of oligonucleotides in order to make sense of antisense. *J. Control. Release* **97**: 189–209

Sorgi, F. L., Bhattacharya, S., Huang, L. (1997) Protamine sulfate enhances lipid-mediated gene transfer. *Gene Ther.* **4**: 961–968

Stephenson, M. L., Zamecnik, P. C. (1978) Inhibition of Rous sarcoma viral RNA translation by a specific oligodeoxyribonucleotide. *Proc. Natl Acad. Sci. USA* **75**: 285–288

Xu, Y., Zhang, H. Y., Thormeyer, D., Larsson, O., Du, Q., Elmen, J., Wahlestedt, C., Liang, Z. (2003) Effective small interfering RNAs and phosphorothioate antisense DNAs have different preferences for target sites in the luciferase mRNAs. *Biochem. Biophys. Res. Commun.* **306**: 712–717

Yamada, Y., Shinohara, Y., Kakudo, T., Chaki, S., Futaki, S., Kamiya, H., Harashima, H. (2005a) Mitochondrial delivery of mastoparan with transferrin liposomes equipped with a pH-sensitive fusogenic peptide for selective cancer therapy. *Int. J. Pharm.* **299**: 34–40

Yamada, Y., Kogure, K., Nakamura, Y., Inoue, K., Akita, H., Nagatsugi, F., Sasaki, S., Suhara, T., Harashima, H. (2005b) Development of efficient packaging method of oligodeoxynucleotides by a condensed nano particle in lipid envelope structure. *Biol. Pharm. Bull.* **28**: 1939–1942

Zamecnik, P. C., Stephenson, M. L. (1978) Inhibition of Rous sarcoma virus replication and cell transformation by a specific oligonucleotide. *Proc. Natl Acad. Sci. USA* **75**: 280–284

# Intracellular Traffic and Fate of Protein Transduction Domains HIV-1 TAT Peptide and Octaarginine. Implications for Their Utilization as Drug Delivery Vectors

Saly Al-Taei,[†,⊥] Neal A. Penning,[†,⊥] Jeremy C. Simpson,[‡] Shiroh Futaki,[§,∥] Toshihide Takeuchi,[§] Ikuhiko Nakase,[§] and Arwyn T. Jones*[,†]

Welsh School of Pharmacy, Cardiff University, Cardiff, CF10 3XF, Wales, United Kingdom, Cell Biology and Biophysics, EMBL-Heidelberg, 69117 Heidelberg, Germany, Institute for Chemical Research, Kyoto University, Uji, Kyoto 611-0011, Japan, and PRESTO, Japan Science and Technology Agency (JST), Kawaguchi, Saitama 332-0012, Japan. Received September 10, 2005; Revised Manuscript Received November 17, 2005

Transduction domains such as those derived from the HIV-TAT protein are candidate vectors for intracellular delivery of therapeutic macromolecules such as DNA and proteins. The mechanism by which they enter cells is controversial, and very little spatial information regarding the downstream fate of these peptides from the plasma membrane is available. We studied endocytic traffic of fluorescent conjugates of HIV-TAT peptide and octaarginine in human hematopoietic cell lines K562 ($CD34^-$) and KG1a ($CD34^+$) and substantiated our findings in epithelia cells. Both peptides were efficiently internalized to endocytic pathways of both hematopoietic cell lines; however, comparative analysis of the intracellular location of the peptides with endocytic probes revealed major differences in spatial organization of their endocytic organelles and their interaction with the peptides at low temperatures. Double labeling confocal microscopy demonstrates that prelabeled lysosomes of all the tested cells are accessible to internalized peptides within 60 min of endocytic uptake. Incubation of cells with nocodazole and cytochalasin D inhibited peptide traffic from early to late endosomal structures, demonstrating a cytoskeletal requirement for lysosomal delivery. Disruption of Golgi and endoplasmic reticulum dynamics was without effect on peptide localization, suggesting that endosomes and lysosomes rather than these organelles are the major acceptor compartments for these molecules.

## INTRODUCTION

Peptides derived from a number of proteins are able to enter cells and gain access to the cytosol and nucleus, thus generating much interest in their potential use as vectors for intracellular delivery of therapeutic molecules (*1*–*4*). To date, the most studied include cationic peptides derived from proteins such as the HIV transcription factor TAT, the *Drosophila melanogaster* homeobox protein Antennapedia (penetratin), and the herpes simplex virus protein VP22. These have been classified as cell penetrating peptides or protein transduction domains (PTD).[1] Predominantly in cell models, these peptides have been shown to have potential as cellular delivery vectors for enhancing the activities of their associated cargo, whether they be small molecules such as cytotoxic drugs or macromolecules such as genes and proteins (*1*, *2*, *5*–*7*). Transition of their use from cell culture systems to animal disease models has been slow, but the ability of TAT conjugates to protect mice against ischemia, to inhibit tumor growth, and enhance gene delivery in aerosol formulations suggests that these offer wide ranging pharmaceutical applications for treating a range of diseases (*2*, *7*–*9*).

Much research has been directed toward understanding how the peptides, either alone or in conjugation with other molecules, traverse biological barriers such as the plasma membrane and those lining endocytic organelles and the nucleus. Recently a number of cellular localization and uptake observations, documented for PTDs in cell culture models, were found to be due to artifacts caused by fixation and extensive nonspecific binding of the peptides to the plasma membrane at physiological and low temperatures (*10*, *11*). Recent data suggest a major role for endocytosis in PTD uptake but an agreed mechanism for their intracellular traffic, following internalization, is yet to emerge (*10*, *12*–*17*).

On the classical endocytic pathway, TAT peptides have been shown to colocalize with markers of early/recycling endosomes such as transferrin and FM4-64 (*10*, *18*). Since TAT–DNA conjugates or complexes have the capacity to modify gene expression, a fraction of the peptides therefore escape, presumably from the endocytic pathway or associated organelles, in an undefined mechanism to the cytosol. Internalized TAT peptides have also been shown to colocalize with the Golgi marker BODIPY-ceramide and in agreement with direct traffic from early endosomes to the Golgi complex, no peptide was visualized in Lysotracker-labeled late endosomes and lysosomes (*14*). These data suggest that the peptides could utilize the retrograde secretory pathway via the Golgi complex and enter the cytosol from the endoplasmic reticulum. Earlier reports have demonstrated that TAT peptide fusion proteins enter neutral caveosomes via plasma membrane caveolae (*13*), but more recent reports suggest that caveolae are not required for uptake

* To whom correspondence should be addressed: Welsh School of Pharmacy, Redwood Building, Cardiff University, Cardiff, CF10 3XF, Wales, United Kingdom. Tel: +44 (0) 2920876431, Fax: +44 (0) 2920874536; E-mail: jonesat@cardiff.ac.uk.

† Cardiff University.

‡ EMBL-Heidelberg.

§ Kyoto University.

∥ PRESTO.

⊥ Both authors contributed equally to this work

[1] Abbreviations: BFA, Brefeldin A; CytD, Cytochalasin D; EEA1, Early Endosome Antigen 1; EIPA, 5-(*N*-ethyl-*N*-isopropyl)amiloride; PI 3-kinase, phosphatidylinositol 3-kinase, PTD, protein transduction domains; TFA, trifluoroacetic acid; TGN, *trans*-Golgi network; TMR, tetramethylrhodamine; TxR-Tf, Texas-Red-transferrin.

10.1021/bc050274h CCC: $33.50 
Published on Web 12/27/2005